LUIZ GUSTAVO HAFEMANN

AN ANALYSIS OF DEEP NEURAL NETWORKS FOR TEXTURE CLASSIFICATION

Dissertation presented as partial requisite to obtain the Master's degree. M.Sc. program in Informatics, Universidade Federal do Paraná.
Advisor: Prof. Dr. Luiz Eduardo S. de Oliveira
Co-Advisor: Dr. Paulo Rodrigo Cavalin

CURITIBA

2014

LUIZ GUSTAVO HAFEMANN

AN ANALYSIS OF DEEP NEURAL NETWORKS FOR TEXTURE CLASSIFICATION

Dissertation presented as partial requisite to obtain the Master's degree. M.Sc. program in Informatics, Universidade Federal do Paraná.
Advisor: Prof. Dr. Luiz Eduardo S. de Oliveira
Co-Advisor: Dr. Paulo Rodrigo Cavalin

CURITIBA

2014

ACKNOWLEDGMENTS

I would like to thank my wife, Renata, for all the love, patience and understanding during the last two years. I also want to thank my parents, for all the support during this time, and during all my life. I would like to thank my research advisor, Dr. Luiz Oliveira, and my co-advisor Dr. Paulo Cavalin, for all the guidance and assistance during this time. Last but not least, I would like to thank Dennis Furlaneto for all the reviews of my dissertation, and for the regular discussions in the coffee area, from where many ideas emerged.

CONTENTS

LIST OF FIGURES vi

LIST OF TABLES vii

RESUMO viii

ABSTRACT x

1 INTRODUCTION 1

1.1 Motivation . . . 2

1.2 Challenges . . . 3

1.3 Objectives . . . 3

1.4 Contributions . . . 4

2 THEORETICAL BACKGROUND 6

2.1 Artificial Neural Networks . . . 6

2.1.1 Artificial Neuron . . . 6

2.1.2 Multi-layer Neural Networks . . . 7

2.1.2.1 Forward Propagation . . . 8

2.1.2.2 Training Objective . . . 9

2.1.2.3 Backpropagation . . . 10

2.1.2.4 Training algorithm . . . 11

2.2 Training Deep Neural Networks . . . 13

2.3 Convolutional Neural Networks . . . 14

2.3.1 Convolutional layers . . . 15

2.3.2 Pooling layers . . . 17

2.3.3 Locally-connected layers . . . 18

2.4 Combining Classifiers . . . 18

2.5 Transfer Learning 19
2.5.1 Transfer Learning in Convolutional Neural Networks 20

3 STATE-OF-THE-ART 22

3.1 Deep learning review on the CIFAR-10 dataset 22
3.1.1 Summary of the CIFAR-10 top results 24

4 METHODOLOGY 27

4.1 Texture datasets 28
4.1.1 Forest Species datasets 28
4.1.2 Writer identification 29
4.1.3 Music genre classification 29
4.1.4 Brodatz texture classification 30
4.1.5 Summary of the datasets 31
4.2 Training Method for CNNs on Texture Datasets 31
4.2.1 Image resize and patch extraction 32
4.2.2 CNN architecture and training 33
4.2.3 Combining Patches for testing 35
4.3 Training Method for Transfer Learning 37

5 EXPERIMENTAL RESULTS 42

5.1 Forest species recognition tasks 42
5.1.1 Classification rates 43
5.1.2 Feature Learning 46
5.1.3 Comparison with the state of the art 47
5.2 Author Identification tasks 49
5.2.1 Classification rates 50
5.2.2 Feature Learning 53
5.2.3 Comparison with the state of the art 53
5.3 Music Genre classification task 54
5.3.1 Classification rates 55

5.3.2 Feature Learning 56
5.3.3 Comparison with the state of the art 57
5.4 Brodatz-32 texture classification task 58
5.4.1 Classification rates 59
5.4.2 Feature Learning 60
5.4.3 Comparison with the state of the art 60
5.5 Transfer Learning 61
5.5.1 Tasks from similar domains 61
5.5.2 Tasks from distinct domains 63

6 CONCLUSION **65**

A SAMPLE IMAGES ON THE DATASETS **66**

BIBLIOGRAPHY **1**

LIST OF FIGURES

2.1 A single artificial neuron. 7
2.2 A neural network composed of three layers. 8
2.3 Architecture of a convolution network for traffic sign recognition [36]. . . . 14
2.4 Sample feature maps learned by a convolution network for traffic sign recognition [36] 15
2.5 The forward propagation phase of a convolutional layer. 16
2.6 The forward propagation phase of a pooling layer. 17
2.7 Transfer learning from the ImagetNet dataset to the Pascal VOC dataset . 21

4.1 An overview of the Pattern Recognition process. 27
4.2 The zoning methodology used by Costa [56]. 30
4.3 The Deep Convolutional Neural Network architecture. 33
4.4 The training procedure using random patches 36
4.5 The testing procedure using non-overlapping patches 38
4.6 The training procedure for transfer learning 40
4.7 The testing procedure for transfer learning 41

5.1 Error rates on the Forest Species dataset with Macroscopic images, for CNNs trained with different hyperparameters. 43
5.2 Error rates on the Forest Species dataset with Microscopic images, for CNNs trained with different hyperparameters. 44
5.3 Random predictions for patches on the Testing set (Macroscopic images) . 45
5.4 Random predictions for patches on the Testing set (Microscopic images) . . 46
5.5 Filters learned by the first convolutional layers of models trained on the Macroscopic images dataset. 47
5.6 Filters learned by the first convolutional layer of a model trained on the Microscopic images dataset. 47

5.7 Error rates on the IAM dataset, for CNNs trained with different hyperparameters. 50
5.8 Error rates on the BFL dataset, for CNNs trained with different hyperparameters. 51
5.9 Random predictions for patches on the IAM Testing set 52
5.10 Random predictions for patches on the BFL Testing set 52
5.11 Filters learned by the first convolutional layer of a model trained on the IAM dataset. 53
5.12 Filters learned by the first convolutional layer of a model trained on the BFL dataset. 53
5.13 Error rates on the Latin Music Dataset, for CNNs trained with different hyperparameters. 55
5.14 Random predictions for test patches on the Latin Music Dataset 56
5.15 Filters learned by the first convolutional layer of a model trained on the Latin Music dataset. 56
5.16 Error rates on the Brodatz dataset, for CNNs trained with different hyperparameters. 59
5.17 Random predictions for patches on the Brodatz-32 Testing set 60
5.18 Filters learned by the first convolutional layer of a model trained on the Brodatz-32 dataset. 60

A.1 Sample images from the macroscopic Brazilian forest species dataset 66
A.2 Sample images from the microscopic Brazilian forest species dataset 67
A.3 Sample texture created from the Latin Music Dataset dataset. 67
A.4 Sample image from the BFL dataset, and the associated texture. [53] . . . 68
A.5 Sample image from the IAM dataset, and the associated texture. [8] 68
A.6 Sample images from the Brodatz-32 dataset [58] 69

LIST OF TABLES

3.1 Comparison of top published results on the CIFAR-10 dataset 26

4.1 Summary of the properties of the datasets 31

5.1 Classification on the Macroscopic images dataset 48
5.2 Classification on the Microscopic images dataset 48
5.3 Classification on the IAM dataset 53
5.4 Classification on the BFL dataset 54
5.5 Classification on the Latin Music dataset 57
5.6 Confusion Matrix on the Latin Music Dataset classification (%) - Our method 58
5.7 Confusion Matrix on the Latin Music Dataset classification (%) - Costa et al.[9] 58
5.8 Classification on the Brodatz-32 dataset 61
5.9 Classification on the Macroscopic Forest species dataset 62
5.10 Classification on the BFL dataset 62
5.11 Classification on the BFL dataset 63
5.12 Classification on the Brodatz-32 dataset 64

RESUMO

Classificação de texturas é um problema na área de Reconhecimento de Padrões com uma ampla gama de aplicações. Esse problema é geralmente tratado com o uso de descritores de texturas e modelos de reconhecimento de padrões, tais como Máquinas de Vetores de Suporte (SVM) e Regra dos K vizinhos mais próximos (KNN).

O método clássico para endereçar o problema depende do conhecimento de especialistas no domínio para a criação de extratores de características relevantes (discriminantes), criando-se vários descritores de textura, cada um voltado para diferentes cenários (por exemplo, descritores de textura que são invariantes rotação, ou invariantes borramento da imagem). Uma estratégia diferente para o problema é utilizar algoritmos para aprender os descritores de textura, ao invés de construí-los manualmente. Esse é um dos objetivos centrais de modelos de Arquitetura Profunda – modelos compostos por múltiplas camadas, que tem recebido grande atenção nos últimos anos. Um desses métodos, chamado de Rede Neural Convolucional, tem sido utilizado para atingir o estado da arte em vários problemas de visão computacional como, por exemplo, no problema de reconhecimento de objetos. Entretanto, esses métodos ainda não são amplamente explorados para o problema de classificação de texturas.

A presente dissertação preenche essa lacuna, propondo um método para treinar Redes Neurais Convolucionais para problemas de classificação de textura, lidando com os desafios e tomando em consideração as características particulares desse tipo de problema. O método proposto foi testado em seis bases de dados de texturas, cada uma apresentando um desafio diferente, e resultados próximos ao estado da arte foram observados para a maioria das bases, obtendo-se resultados superiores em duas das seis bases de dados.

Por fim, é apresentado um método para transferência de conhecimento entre diferentes problemas de classificação de texturas, usando Redes Neurais Convolucionais. Os experimentos conduzidos demonstraram que essa técnica pode melhorar o desempenho dos classificadores em problemas de textura com bases de dados pequenas, utilizando o

conhecimento aprendido em um problema similar, que possua uma grande base de dados.

Palavras chave: Reconhecimento de padrões; Classificação de Texturas; Redes Neurais Convolucionais

ABSTRACT

Texture classification is a Pattern Recognition problem with a wide range of applications. This task is commonly addressed using texture descriptors designed by domain experts, and standard pattern recognition models, such as Support Vector Machines (SVM) and K-Nearest Neighbors (KNN).

The classical method to address the problem relies on expert knowledge to build relevant (discriminative) feature extractors. Experts are required to create multiple texture descriptors targeting different scenarios (e.g. features that are invariant to image rotation, or invariant to blur). A different approach for this problem is to learn the feature extractors instead of using human knowledge to build them. This is a core idea behind Deep Learning, a set of models composed by multiple layers that are receiving increased attention in recent years. One of these methods, Convolutional Neural Networks, has been used to set the state-of-the-art in many computer vision tasks, such as object recognition, but are not yet widely explored for the task of texture classification.

The present work address this gap, by proposing a method to train Convolutional Neural Networks for texture classification tasks, facing the challenges of texture recognition and taking advantage of particular characteristics of textures. We tested our method on six texture datasets, each one posing different challenges, and achieved results close to the state-of-the-art in the majority of the datasets, surpassing the best previous results in two of the six tasks.

We also present a method to transfer learning across different texture classification problems using Convolutional Neural Networks. Our experiments demonstrated that this technique can improve the performance on tasks with small datasets, by leveraging knowledge learned from tasks with larger datasets.

Keywords: Pattern Recognition; Texture Classification; Convolutional Neural Networks

CHAPTER 1

INTRODUCTION

Texture classification is an important task in image processing and computer vision, with a wide range of applications, such as computer-aided medical diagnosis [1], [2], [3], classification of forest species [4], [5], [6], classification in aerial/satellite images [7], writer identification and verification [8] and music genre classification [9].

Texture classification commonly follows the standard procedure for pattern recognition, as described by Bishop et al. in [10]: extract relevant features, train a model using a training dataset, and evaluate the model on a held-out test set.

Many methods have been proposed for the feature extraction phase on texture classification problems, as reviewed by Zhang et al. [11] and tested on multiple datasets by Guo et al. [12]. Noteworthy techniques are: Gray-Level Co-occurrence Matrices (GLCM), the Local Binary Pattern operator (LBP), Local Phase Quantization (LPQ), and Gabor filters.

The methods above rely on domain experts to build the feature extractors to be used for classification. An alternative approach is to use models that learn directly from *raw* data, for instance, directly from pixels in the case of images. The intuition is using such methods to learn multiple intermediate representations of the input, in layers, in order to better represent a given problem. Consider an example for object recognition in an image: the inputs for the model can be the raw pixels in the image. Each layer of the model constitutes an equivalent of *feature detectors*, transforming the data into more abstract (and hopefully useful) representations. The initial layers can learn low-level features, such as detecting edges, and subsequent layers learn higher-level representations, such as detecting more complex local shapes, up to high-level representations, such as recognizing a particular object [13]. In summary, the term Deep Learning refers to machine learning models that have multiple layers, and techniques for effectively training these models,

commonly building Deep Neural Networks or Deep Belief Networks [14], [15].

Methods using deep architectures have set the state-of-the-art in many domains in recent years, as reviewed by Bengio in [13] and [16]. Besides improving the accuracy on different pattern recognition problems, one of the fundamental goals of Deep Learning is to move machine learning towards the automatic discovery of multiple levels of representation, reducing the need for feature extractors developed by domain experts [16]. This is especially important, as noted by Bengio in [13], for domains where the features are hard to formalize, such as for object recognition and speech recognition tasks.

In the task of object recognition, deep architectures have been widely used to achieve state-of-the-art results, such as in the CIFAR dataset[17] where the top published results use Convolutional Neural Networks (CNN) [18]. The tasks of object and texture classification present similarities, such as the strong correlation of pixel intensities in the 2-D space, and present some differences, such as the ability to perform the classification using only a relatively small fragment of a texture. In spite of the similarities with object classification we observe that deep learning techniques are not yet widely used for texture classification tasks. Kivinen and Williams [19] used Restricted Boltzmann Machines (RBMs) for texture synthesis, and Luo et al. [20] used spike-and-slab RBMs for texture synthesis and inpainting. Both consider using image pixels as input, but they do not consider training deep models for classification among several classes. Titive et al. [21] used convolutional neural networks on the Brodatz texture dataset, but considered only low resolution images, and a small number of classes.

The similarities between texture classification and object recognition, and the good results demonstrated by using deep architectures for object recognition suggest that these techniques could be successfully applied for texture classification.

1.1 Motivation

There is a considerable set of potential applications for texture recognition, as briefly presented above. However, despite the reported success of classical texture classification techniques in many of these tasks, these problems are still not resolved and are subject

of active research, with potential to increase recognition rates.

A second motivation is that traditional machine learning techniques often require human expertise and knowledge to hand-engineer features, for each particular domain, to be used in classification and regression tasks. It can be considered that the actual intelligence in such systems is therefore in the creation of such features, instead of the machine learning algorithm that uses them. Therefore, using techniques that do not rely on expert-defined feature extractors can make it easier to develop effective machine learning models for novel datasets, without requiring the test and selection of a large set of possible feature extractors.

1.2 Challenges

Here is a set of challenges in applying deep learning techniques to texture classification problems:

- Image size: The majority of the image-related tasks where deep learning was successfully applied used images of small size. Examples: MNIST (28x28 pixels), STL-10 (96x96), Norb (108x108), Cifar-10 and Cifar-100 (32x32).

- Model size and Training time: One exception to dataset list above is the ImageNet dataset, which consists in high-resolution images of variable sizes. The best results on this dataset, however, require significant usage of computer resources (such as 16 thousands cores running for three days [22]). The texture datasets commonly consist of higher resolution images, and therefore different techniques need to be tested, in order to classify the textures without using too much computing resources.

1.3 Objectives

The main objective of this research is to test whether or not deep learning models, in particular Convolutional Neural Networks, can be successfully applied for texture classification problems.

More specifically, we test these methods on multiple texture datasets, developing a method to cope with the high-resolution texture images without requiring models that are too large, or that require too much computing power to train. Six texture datasets were selected for testing, representing different domain problems, and containing different characteristics, such as image sizes, number of classes and number of samples per class. As part of this effort, we assess if it is possible to obtain a generic framework that brings good results for multiple texture problems.

After training the models on each dataset, the accuracy of the deep models are compared with the state-of-the-art results achieved using the classical texture descriptors.

Finally, another objective of this research is to evaluate a method of Transfer Learning for texture classification. Transfer Learning consists in using a model trained in one task to improve results on another task. This is particularly interesting when using Deep Neural Networks, as these models often require large datasets to be effectively trained. We investigate the hypothesis that we can leverage a neural network trained on a large dataset to improve the results on other tasks, including tasks with smaller datasets.

1.4 Contributions

In this dissertation, we propose a method to train Convolutional Neural Networks on texture classification datasets. We explore the hypothesis that, for most textures, we can classify a texture using only a small fragment of the image. This allowed us to use datasets with large images and still keep the neural network models with a reasonable size. It also enabled us to use a strategy of classifying parts of the images individually, and subsequently combine the results of multiple predictions of the same texture image, achieving good results. We validated our method using six texture datasets, each one posing different challenges. The proposed method obtained excellent results for some types of tasks (in particular, tasks with large datasets), achieving state-of-the-art performance.

We also propose a method to transfer learning across texture classification tasks, using a Convolutional Neural Network. We explore the idea that the weights learned by a Convolutional Neural Network can be used similarly to feature extractors, evaluating the

hypothesis that the features learned by the model in one dataset can be relevant for other tasks. We explore this idea by using a CNN trained in one dataset to improve the performance on a task with another dataset. We validated this proposal in four experiments, considering both cases where the tasks are from similar domains, and cases where the tasks are from different domains. We found that the method for transfer learning was particularly useful to improve the performance on tasks with small datasets, even when transfer knowledge to a task from a different domain.

The remainder of this dissertation is organized as follows. We present the theoretical background of neural networks and transfer learning in Chapter 2. In Chapter 3 we review the state-of-the-art of using deep neural networks for a similar task: object recognition. In Chapter 4, we present our method for training CNNs for texture classification, and the method to transfer learning across texture classification tasks. The experimental evaluation is presented in Chapter 5, and we conclude our work in Chapter 6. Appendix A lists samples from the texture datasets used in the experimental evaluation.

CHAPTER 2

THEORETICAL BACKGROUND

To make this document self-contained, this Chapter reviews the theoretical foundations for Deep Neural Networks. The basic concepts of Artificial Neural Networks are presented, starting with the original models that date back from 1943. The concept of Deep Neural networks is then reviewed, with the recent advancements in the field that enabled training Deep Neural Networks successfully. Afterwards, we review the theoretical foundations of other procedures and methods used in the present work: the combination of multiple classifiers, and transferring knowledge across different learning tasks.

2.1 Artificial Neural Networks

Artificial Neural Networks are mathematical models that use a collection of simple computational units, called Neurons, interlinked in a network. These models are used in a variety of pattern recognition tasks, such as speech recognition, object recognition, identification of cancerous cells, among others [23]

Artificial Neural Networks date back to 1943, with work by McCulloch and Pitts [24]. The motivation for studying neural networks was the fact that the human brain was superior to a computer at many tasks, a statement that holds true even today for tasks such as recognizing objects and faces, in spite of the huge advances in the processing speed in modern computers.

2.1.1 Artificial Neuron

The neuron is the basic unit on Artificial Neural Networks, and it is used to construct more powerful models. A typical set of equations to describe Neural Networks is provided in [25], and is listed below for completeness. A single neuron implements a mathematical function given its inputs, to provide an output, as described in equation 2.1 and illustrated

Figure 2.1.

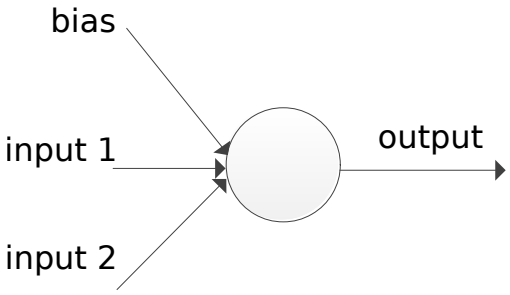

Figure 2.1: A single artificial neuron.

$$f(x) = \sigma(\sum_{i=1}^{n} x_i w_i + b) \tag{2.1}$$

In this equation, x_i is the input i, w_i is the weight associated with input i, b is a bias term and σ is a non-linear function. Common non-linear functions are the sigmoid function (described in 2.2), and the Hyperbolic tangent function ($tanh$).

$$\sigma(x) = \frac{1}{1 + e^{-x}} \tag{2.2}$$

More recently, a new and simple type of non-linearity has been proposed, called Rectified Linear Units (ReLU). Tests conducted by Krizhevsky in [26] reported convergence 6 times faster by using ReLU activations compared to equivalent networks with $tanh$ units. This non-linearity is described in equation 2.3

$$\sigma(x) = max(0, x) \tag{2.3}$$

2.1.2 Multi-layer Neural Networks

Models based on a single neuron, also called Perceptrons, have severe limitations. As noted by Minsky and Papert [27], a perceptron cannot model data that is not linearly separable, such as modelling a simple XOR operator. On the other hand, as shown by Hornik et al. [28], Multi-layer Neural Networks are universal approximators, that is: they can approximate any measurable function to any desired degree of accuracy.

A Multi-layer Neural network consists of several layers of neurons. The first layer is composed of the inputs to the neural network, it is followed by one or more *hidden* layers, up to a last layer that contains the outputs of the network. In the simplest configuration, each layer l is fully connected with the adjacent layers ($l-1$ and $l+1$), and produces an output vector y^l given the output vector of the previous layer y^{l-1}. The output of a layer is calculated by applying the neuron activation function for all neurons on the layer, as noted in equation 2.4, where W^l is a matrix of weights assigned to each pair of neurons from layer l and $l-1$, and b^l is a vector of bias terms for each neuron in layer l.

$$y^l = \sigma(W^l y^{l-1} + b^l) \tag{2.4}$$

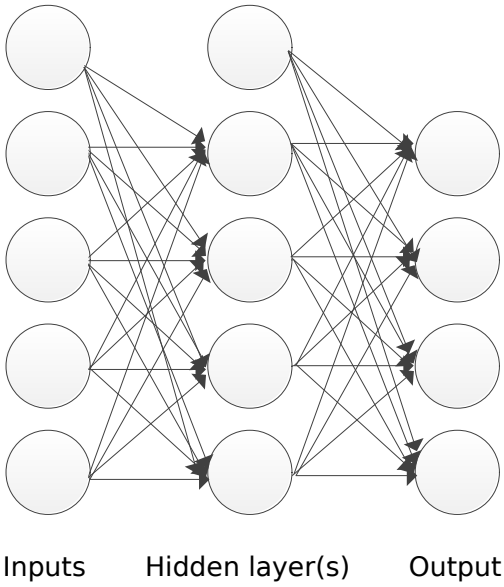

Figure 2.2: A neural network composed of three layers.

2.1.2.1 Forward Propagation

The phase called *forward propagation* consists in applying the neuron activation equation (2.1) starting from first hidden layer, up to the output layer. For classification tasks, the output layer commonly uses another activation function, called **Softmax**. Softmax is particularly useful for the last layer as the function generates a well-formed probability distribution on the outputs. The softmax equation is defined below (2.5 and 2.6). In

these equations, z_i^l is the output of the layer (for neuron i) before the application of the non-linearity, y_i^l is the output of the layer for the neuron i, W_i^l is a vector of weights connecting each neuron on layer $l-1$ to the neuron i on layer l and b_i^l is a bias term for the neuron. The summation term considers all neurons j on the layer l.

$$z_i^l = W_i^l y^{l-1} + b_i^l \tag{2.5}$$

$$y_i^l = \frac{e^{z_i^l}}{\sum_j e^{z_j^l}} \tag{2.6}$$

2.1.2.2 Training Objective

In order to train the model, an **error function**, also called **loss function**, is defined. This function calculates the error of the model predictions with respect to a dataset. The objective of the training is to minimize the sum (or, equivalently, minimize the mean) of this error function applied to all examples in the dataset. Commonly used loss functions are the Squared Error function (SE), described in equation 2.7, and the Cross-Entropy error function (CE), described in equation 2.8 (both equations describe the error for a single example in the dataset). As analyzed by Golik et al [29], it can be shown that the true posterior probability is a global minimum for both functions, and therefore a Neural Network can be trained by minimizing either. On the other hand, in practice using Cross-Entropy error leads to faster convergence, and therefore this error function became more popular in recent years.

$$E = \frac{1}{2} \sum_c (y_c^l - t_c)^2 \tag{2.7}$$

$$E = -\sum_c (t_c \log y_c^l)^2 \tag{2.8}$$

In these equations, y_c^l is the output of unit c in the last layer in the model (l), and t_c is the identity function applied to the true label t (refer to equation 2.9):

$$t_c = \begin{cases} 1, & \text{if } t = c \\ 0, & \text{otherwise} \end{cases} \tag{2.9}$$

2.1.2.3 Backpropagation

The error function can be minimized using Gradient-Based Learning. This strategy consists in taking partial derivatives of the error function with respect to the model parameters, and using these derivatives to iteratively update the parameters [30]. Efficient learning algorithms can be used for this purpose if these gradients (partial derivatives) can be computed analytically.

The phase called *backpropagation* consists in calculating the derivatives of the error function with respect to the model's parameters (weights and biases), by propagating the error from the output layers, back to the initial layers, one layer at a time. Since each layer in the Neural Network consists of simple functions using only the values from the previous layer, we can use the chain rule to easily determine the derivatives analytically. For instance, to calculate the gradient respective to the weights in a layer we have the equation below, as described in [31]:

$$\frac{\delta E}{\delta w_{hj}} = \frac{\delta E}{\delta y_i} \frac{\delta y_i}{\delta z_h} \frac{\delta z_h}{\delta w_{hj}} \tag{2.10}$$

Where y_i is the output of the neuron, z_h is the output before applying the activation function, and w_{hj}'s are the weights.

In order to use this strategy, we need to calculate:

1. The derivative of the error with respect to the neurons in the last layer $\frac{\delta E}{\delta y_i^L}$
2. The derivative of the outputs y_i with respect to the outputs before the activation function z_i, that is $\frac{\delta y_i^l}{\delta z_i^l}$
3. The derivative of z_j with respect to the weights w_{ij}, that is $\frac{\delta z_j^l}{\delta w_{i,j}^l}$
4. The derivative of z_j with respect to the bias b_j, that is $\frac{\delta z_j^l}{\delta b_j^l}$

5. The derivative of z_j with respect to its inputs, that is $\frac{\delta z_j^l}{\delta y_i^{l-1}}$

We start with the top layer, calculating the derivative of the error (Cross-Entropy) with respect to z_i. In this equation, t_i is defined as above (in equation 2.9):

$$\frac{\delta E}{\delta z_i^l} = y_i^l - t_i \tag{2.11}$$

For the derivatives with respect to the weights, we obtain the formula:

$$\frac{\delta z_j^l}{\delta w_{ij}^l} = y_i^{l-1} \tag{2.12}$$

For the derivatives with respect to the biases, we obtain the formula:

$$\frac{\delta z_j^l}{\delta b_i^l} = 1 \tag{2.13}$$

For the derivatives with respect to the inputs, we obtain the formula:

$$\frac{\delta z_j^l}{\delta y_i^{l-1}} = w_{ij}^l \tag{2.14}$$

The equations above are sufficient to compute the derivatives with respect to the weights and biases of the last layer, and the derivative with respect to the outputs of the layer $l-1$. The other equation necessary is the derivative of the activation function of the layers 1 until $l-1$ (that don't use softmax). The derivative for the sigmoid function is described below:

$$\frac{\delta y_i^l}{\delta z_i^l} = y_i^l(1 - y_i^l) \tag{2.15}$$

2.1.2.4 Training algorithm

Training the network consists in minimizing the error function (by updating the weights and biases), often using the Stochastic Gradient Descent algorithm (SGD), or quasi-Newton methods, such as L-BFGS (Limited memory Broyden-Fletcher-Goldfarb-Shanno

algorithm).

The SGD algorithm, as defined in [32], is described below at a high-level. The inputs are: W - the weights and biases of the network, (X, y) - the dataset, *batch_size* - the number of training examples that are used in each iteration, and α, the learning rate. For notation simplicity, all the model parameters are represented in W. In practice, each layer usually defines a 2-dimensional weight matrix and a 1-dimensional bias vector. In summary, SGD iterates over mini-batches of the dataset, performing forward-propagation followed by a back-propagation to calculate the error derivatives with respect to the parameters. The weights are updated using these derivatives and a new mini-batch is used. This procedure is repeated until a convergence criterion is reached. Common convergence criteria are: a maximum number of *epochs* (number of times that the whole training set was used); a desired value for the cost function is reached; or training until the cost function shows no improvement in a number of iterations.

Algorithm 1 Stochastic Gradient Descent

Require: W, X, y, *batch_size*, α

  $W \leftarrow$ random values

  repeat

    x_batch, $y\_batch \leftarrow$ next *batch_size* examples in (X, y)

    $network\_state \leftarrow$ **ForwardProp**(W, x_batch)

    $W_{grad} \leftarrow$ **BackProp**($network\_state$, y_batch)

    $\Delta W \leftarrow -\alpha W_{grad}$

    $W \leftarrow W + \Delta W$

  until Convergence_Criteria()

One of the potential problems with stochastic gradient descent is having oscillations in the gradient, since not all examples are used for each calculation of the derivatives. This can cause slow convergence of the network. One strategy to mitigate this problem is the use of *Momentum*. The idea is to take the running average of the derivatives, by incorporating the previous update ΔW in the update for the current iteration. The equation for momentum is defined in equation 2.16 [31]. In this equation Δw^t refers to

the update to the weights in iteration t, and β is a factor for the momentum, usually taken between 0.5 and 1.0 [31].

$$\Delta w_{ij}^{(t)} = -\alpha \frac{\delta E^{(t)}}{\delta w_i} + \beta \Delta w_{ij}^{(t-1)} \tag{2.16}$$

2.2 Training Deep Neural Networks

The depth of an architecture refers to the number of non-linear operations that are composed on the network. While many of the early successful applications of neural networks used shallow architectures (up to 3 levels), the mammal brain is organized in a deep architecture. The brain appears to process information through multiple stages, which is particularly clear in the primate visual system[13]. Deep Neural Networks have been investigated for decades, but training deep networks consistently yielded poor results, until very recently. It was observed in many experiments that deep networks are harder to train than shallow networks, and that training deep networks often get stuck in apparent local minima (or plateaus) when starting with random initialization of the network parameters. It was discovered, however, that better results could be achieved by pre-training each layer with an unsupervised learning algorithm [14]. In 2006, Hinton obtained good results using Restricted Boltzmann Machines (a generative model) to perform unsupervised training of the layers [14]. The goal of this training was to obtain a model that could capture patterns in the data, similarly to a feature descriptor, not using the dataset labels. The weights learned by this unsupervised training were then used to initialize neural networks. Similar results were reported using auto-encoders for training each layer [15]. These experiments identified that layers could be pre-trained one at a time, in a greedy layer-wise format. After the layers are pre-trained, the learned weights are used to initialize the neural network, and then the standard back-propagation algorithm is used for fine-tuning the network. The advantage of unsupervised pre-training was demonstrated in several statistical comparisons [15], [33], [34], until recently, when deep neural networks trained only with supervised learning started to register similar results in some tasks (like object recognition). Ciresan et al. [18] demonstrate that properly trained deep neural networks

(with only supervised learning) are able to achieve top results in many tasks, although not denying that pre-training might help, especially in cases were little data is available for training, or when there are massive amounts of unlabeled data.

On the task of image classification, the best published results use a particular type of architecture called *Convolutional Neural Network*, which is described in the next section.

2.3 Convolutional Neural Networks

Convolutional networks combine three architectural ideas: local receptive fields, shared (tied) weights and spatial or temporal sub-sampling [30]. This type of network was used to obtain state-of-the-art results in the CIFAR-10 object recognition task [18] and, more recently, to obtain state-of-the-art results in more challenging tasks such as the ImageNet Large Scale Visual Recognition Challenge [35]. For both tasks, the training process benefited from the significant speed-ups on processing using modern GPUs (Graphical Processing Units), which are well suited for the implementation of convolutional networks.

The following sections describe the types of layers that compose a Convolutional Neural Network. To illustrate the concept, Figure 2.3 shows a sample Convolutional Network.

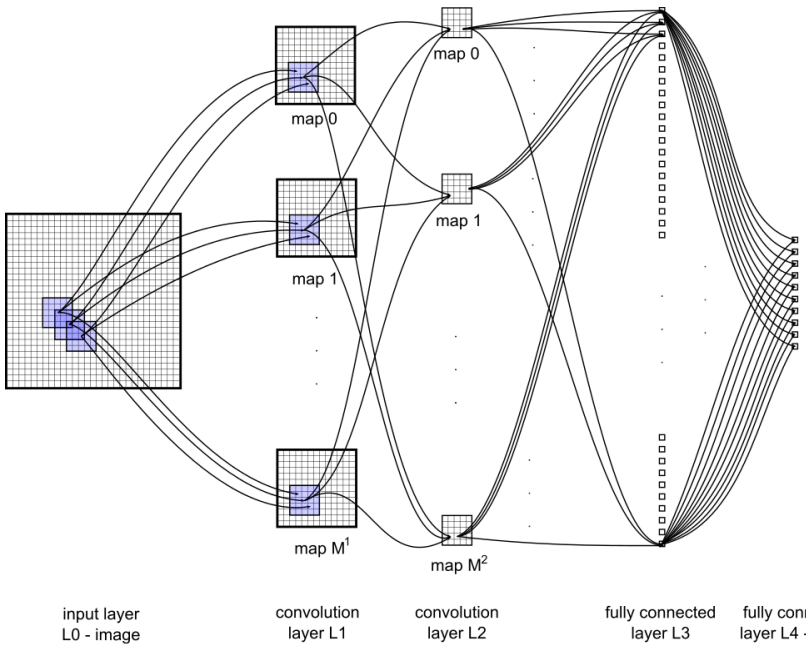

Figure 2.3: Architecture of a convolution network for traffic sign recognition [36].

Figure 2.4 provides an example of the filters learned on the first convolutional layer of a network trained for traffic sign recognition, showing that this type of architecture is capable of learning interesting feature detectors, similar to edge detectors.

Figure 2.4: Sample feature maps learned by a convolution network for traffic sign recognition [36]

2.3.1 Convolutional layers

Convolutional layers have trainable *filters* (also called *feature maps*) that are applied across the entire input[37]. For each filter, each neuron is connected only to a subset of the neurons in the previous layer. In the case of 2D input (such as images), the filters define a small area (e.g. 5x5 or 8x8 pixels), and each neuron is connected only to the nearby neurons (in this area) in the previous layer. The weights are shared across neurons, leading the filters to learn frequent patterns that occur in any part of the image.

The definition for a 2D convolution layer is presented in Equation 2.17. It is the application of a discrete convolution of the inputs y^{l-1} with a filter ω^l, adding a bias b^l, followed by the application of a non-linear function σ:

$$y_{rc}^{l} = \sigma(\sum_{i=1}^{F_r}\sum_{j=1}^{F_c} y_{(r+i-1)(c+j-1)}^{l-1} w_{ij}^{l} + b^{l}) \tag{2.17}$$

In this equation, y_{rc}^{l} is the output unit at $\{r, c\}$, F_r and F_c are the number of rows and columns in the 2D filter, w_{ij}^{l} is the value of the filter at position $\{i, j\}$, $y_{(r+i-1)(c+j-1)}^{l-1}$ is the value of input to this layer, at position $\{r+i-1, c+j-1\}$, and b^{l} is the bias term. The forward propagation phase of a convolutional layer is illustrated in figure 2.5.

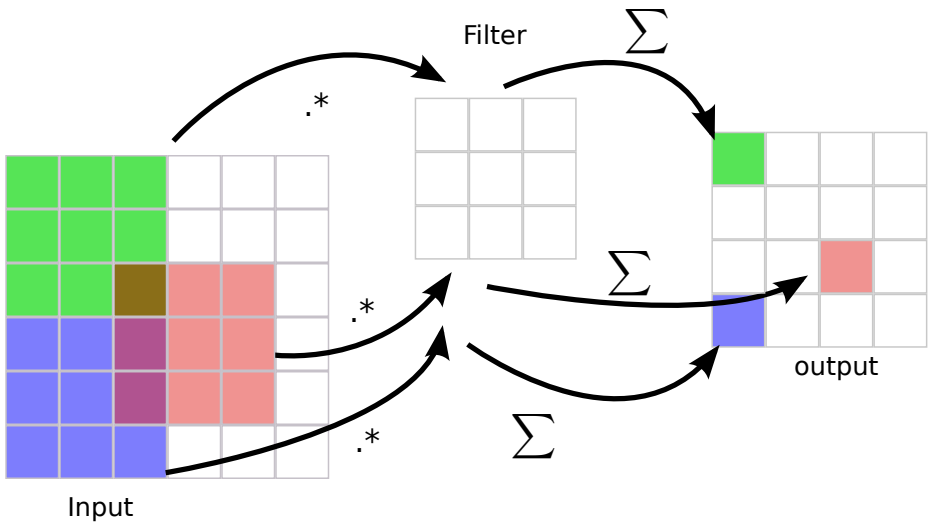

Figure 2.5: The forward propagation phase of a convolutional layer.

The equation above is defined for all possible applications of the filter, that is, for $r \in \{1, ..., X_r - F_r + 1\}$ and $c \in \{1, ..., X_c - F_c + 1\}$, where X_r and X_c are the number of rows and columns in the input to this layer. The convolutional layer can either apply the filters for all possible inputs, or use a different strategy. Mainly to reduce computation time, instead of applying the filter for all possible $\{r, c\}$ pairs, only the pairs with distance s are used, which is called the *stride*. A stride $s = 1$ is equivalent to apply the convolution for all possible pairs, as defined above.

The inspiration for convolutional layers originated from models of the mammal visual system. Modern research in the physiology of the visual system found it consistent with the processing mechanism of convolutional neural networks, at least for quick recognition of objects [13]. Although being a biological plausible model, the theoretical reasons for the success of convolutional networks are not yet fully understood. One hypothesis is

that the small fan-in of the neurons (i.e. the number or input connections to the neurons) helps the derivatives to propagate through many layers - instead of being diffused in a large number of input neurons.

2.3.2 Pooling layers

The pooling layers implement a non-linear downsampling function, in order to reduce dimensionality and capture small translation invariances. Equation 2.18 presents the formulation of one type of pooling layer, max-pooling:

$$y_{rc}^{l} = \max_{i,j \in \{0,1,\ldots,m\}} y_{(r+i-1)(c+j-1)}^{l-1} \tag{2.18}$$

In this equation, y_{rc}^{l} is the output for index $\{r, c\}$, m is the size of the pooling area, and $y_{(r+i-1)(c+j-1)}^{l-1}$ is the value of the input at the position $\{r+i-1, c+j-1\}$. Similarly for the convolutional layer described above, instead of generating all possible pairs of $\{i, j\}$, a stride s can be used. In particular, a stride $s = 1$ is equivalent to using all possible pooling windows, and a stride $s = m$ is equivalent of using all non-overlapping pooling windows. Figure 2.6 illustrates a max-pooling layer with stride=1.

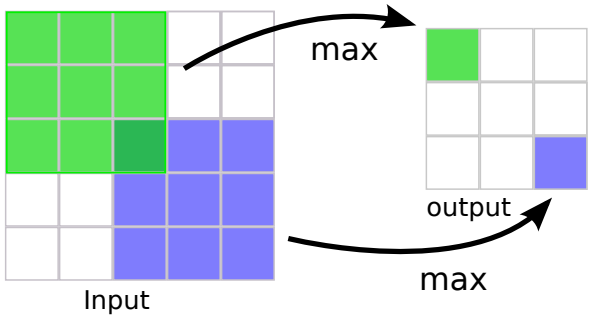

Figure 2.6: The forward propagation phase of a pooling layer.

Scherer et al. [38] evaluated different pooling architectures, and note that the max-pooling layers obtained the best results. Pooling layers add robustness to the model, providing a small degree of translation invariance, since the unit activates independently on where the image feature is located within the pooling window [16]. Empirically, pooling has demonstrated to contribute to improved classification accuracy for object recognition [37].

2.3.3 Locally-connected layers

Locally-connected layers only connect neurons within a small window to the next layer, similarly to convolutional layers, but without sharing weights. The motivation for this type of layer is to achieve something similar to one of the benefits of convolutional layers: to reduce the fan-in of the neurons (the number of input connections to each neuron), enabling the derivatives to propagate through more layers instead of being diffused.

$$y_{rc}^{l} = \sigma(\sum_{i=1}^{m}\sum_{j=1}^{m} W_{ij}^{l,rc} y_{(r+i-1)(c+j-1)}^{l-1}) \tag{2.19}$$

Where: $W_{ij}^{l,rc}$ is the weight associated with layer l, producing the output unit r, c at position i, j, and $y_{(r+i-1)(c+j-1)}^{l-1}$ is the input at position $(r+i-1), (c+j-1)$.

2.4 Combining Classifiers

We now provide an overview of a strategy used in the present work - the combination of multiple classifiers.

One strategy to increase the performance of a pattern recognition system is to, instead of relying on a single classifier, use a combination of multiple classifiers. This is particularly useful when the errors of different classifiers do not completely overlap - suggesting that these classifiers offer complementary information on the examples. Several strategies can be used for creating such classifiers, such as using different feature sets, different training sets, etc. [39].

Kittler et al. [39] provide a theoretical framework for combining classifiers, showing different assumptions (on the classifiers' properties), under which common combination techniques can be derived. The equations for the two most used combination strategies are shown below, simplified for the case where the classes have equal priors:

The **Product rule** is defined in equation 2.20. It combines the classifiers under the assumption that they are conditionally independent.

$$\text{assign Z } \rightarrow \omega_j \text{ if}$$
$$\prod_{i=1}^{R} p(x_i|\omega_j) = \max_{k=1}^{m} \prod_{i=1}^{R} p(x_i|\omega_k) \tag{2.20}$$

In this equation, Z is the pattern being classified, ω_k are the different classes, and $p(x_i|\omega_k)$ is the probability assigned to class k by the classifier i.

The **Sum rule** is defined in equation 2.21. It combines the classifiers under the assumption that the classifiers will not deviate dramatically from the prior probabilities.

$$\text{assign Z } \rightarrow \omega_j \text{ if}$$
$$\sum_{i=1}^{R} p(x_i|\omega_j) = \max_{k=1}^{m} \sum_{i=1}^{R} p(x_i|\omega_k) \tag{2.21}$$

Similar to the equation above, Z is the pattern being classified, ω_k are the different classes, and $p(x_i|\omega_k)$ is the probability assigned to class k by the classifier i.

2.5 Transfer Learning

Transfer learning is a strategy that aims to improve the performance on a machine learning task by leveraging knowledge obtained from a different task. The intuition is: we expect that by learning one task we gain knowledge that could be used to learn similar tasks. For example, learning to recognize apples might help in recognizing pears, or learning to play the electronic organ may help learning the piano [40].

In a survey on transfer learning, Pan and Yang [40] use the following notations and definitions for transfer learning: A **domain** $\mathcal{D}$ consists of two components: a **feature space** $\mathcal{X}$ and a **probability distribution** $P(X)$, where $X = \{x_1, ..., x_n\} \in \mathcal{X}$. Given a specific domain, $\mathcal{D} = \{\mathcal{X}, P(X)\}$, a **task** consist of two components: a label space $\mathcal{Y}$ and an objective predictive function $f(.)$, denoted by $\mathcal{T} = \{\mathcal{Y}, f(.)\}$), which is not observed, but that can be learned from training data. The function $f(.)$ can then be used to predict

the corresponding label, $f(x)$ of a new instance x. From a probabilistic perspective, $f(x)$ can be written as $P(y|x)$. In an example in the texture classification domain, we use a feature descriptor on the textures to generate the feature space $\mathcal{X}$. A given training sample is denoted by X, $X \in \mathcal{X}$, with associated label y, $y \in \mathcal{Y}$. A model is then trained on a dataset to learn the function $f(.)$ (or $P(y|x)$).

With this notation, transfer learning can be defined as follows:

Definition 2.5.1 *Given a source domain $\mathcal{D}_S$ and learning task $\mathcal{T}_S$, a target domain $\mathcal{D}_T$ and learning task $\mathcal{T}_T$, transfer learning aims to help improve the learning of the target predictive function $f_T(.)$ in $\mathcal{D}_T$ using the knowledge in $\mathcal{D}_S$ and $\mathcal{T}_S$, where $\mathcal{D}_S \neq \mathcal{D}_T$, or $\mathcal{T}_S \neq \mathcal{T}_T$*

To illustrate, we can use this definition for texture classification. We can apply transfer learning by using a source task from a different domain $\mathcal{D}$, for example, using a different feature space $\mathcal{X}$ (with a different feature descriptor) or using a dataset with different marginal probabilities $P(X)$ (i.e. textures that display different properties from the target task). We can also apply transfer learning if the task $\mathcal{T}$ is different: for example, using a source task that learns different labels $\mathcal{Y}$ or with different objective $f(.)$.

2.5.1 Transfer Learning in Convolutional Neural Networks

The architecture of state-of-the-art Convolutional Neural Networks (CNN) often contains a large number of parameters, such as the network of Krizhevsky et. al for the ImageNet dataset [26] with 60 million parameters. In this case, the weights are learned from a dataset containing 1.2 million high-resolution images for training. However, directly learning so many parameters from only a few thousand examples is problematic. Transfer learning can assist in this task, by using the internal representation learned from one task, and applying it to another task. As noted by Oquab et. al [41], a CNN can act as a generic extractor of mid-level representations, which can be pre-trained in a source task, and then re-used in other target tasks.

One difficulty to apply this method is that the distribution of the images, $P(X)$, may

differ significantly between the source and target tasks. Oquab et. al [41] propose a simple method to cope with this problem, by training an adaptation layer (using the target dataset), after the convolutional layers are learned in the source task. This process is illustrated in Fig 2.7: first a convolutional neural network is trained in the source task (in their case the ImageNet dataset). The parameters learned by network (except for the last layer) are then transferred to the target task (which has a smaller dataset). To compensate for the different distribution of the images, two fully-connected layers are added to the network, and these two layers are then trained using the target dataset. Using this simple transfer learning procedure, Oquab et. al were able to achieve state-of-the-art results on the competitive Pascal VOC dataset.

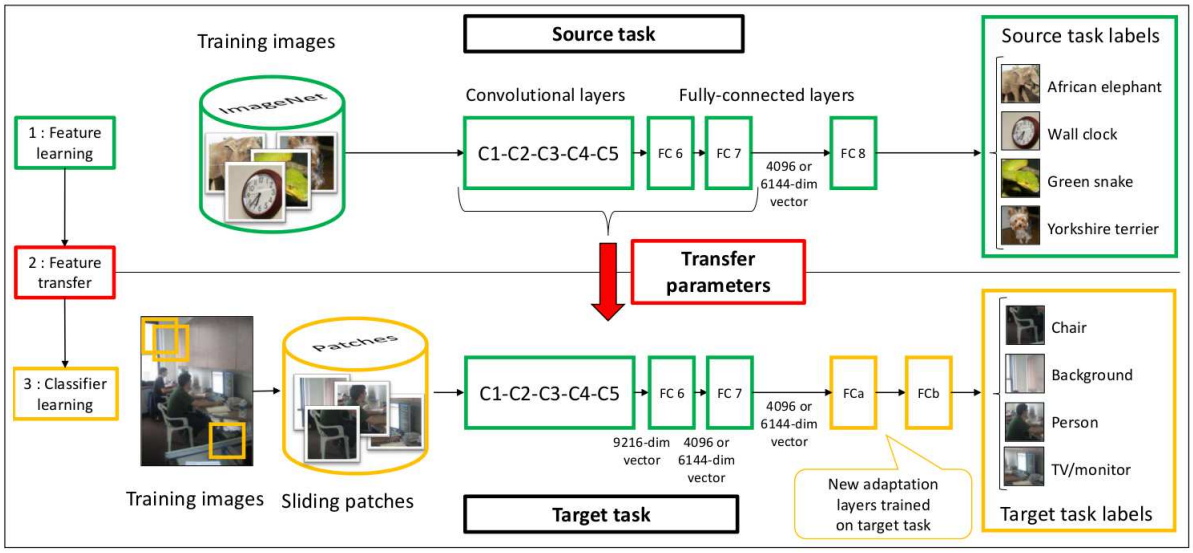

Figure 2.7: Transfer learning from the ImagetNet dataset to the Pascal VOC dataset

CHAPTER 3

STATE-OF-THE-ART

This Chapter reviews the state-of-the-art for Deep Neural Networks applied to a classification task. Deep models were already successfully used in many domains, including several classification tasks [33], [42], [18], natural language processing [43], acoustic modelling in speech recognition[44] , among others. The present work is focused on texture classification, and therefore we limited the analysis for image recognition tasks. In particular, one object recognition problem was selected (CIFAR-10) for comparative analysis. The best published results on this dataset are compared, and their similarities are identified.

3.1 Deep learning review on the CIFAR-10 dataset

Deep learning has been a focus of recent research, and a large variety of models have been proposed in recent years [13]. To support the decisions on which strategies to pursue for texture classification, a survey was conducted on the top published results in an object recognition task: CIFAR-10 [17]. Several similarities were found in the models and methodologies used in these papers, which provided insights for the texture classification task. The detailed results of this analysis can be found below, and it is summarized in the next section.

Goodfellow et al. [45] achieved the best published result on the CIFAR-10 dataset. They used an architecture of three convolutional-layers (each followed by a max-pooling layer), followed by one fully-connected layer, and one fully-connected softmax layer. The key difference on this work is the usage of a new type of neuron, called Maxout, instead of using the sigmoid function. A single maxout neuron can approximate any convex function, and in practice the maxout networks not only learn the relationships between hidden neurons, but also the activation function of each neuron. Their model also made usage of a regularization technique called dropout [46], which is described below. With this archi-

tecture, an accuracy of 90.65% was achieved in this 10-class classification problem. This result was achieved by augmenting the training dataset with translations and horizontal reflections, and using standard preprocessing techniques: Global contrast normalization, and ZCA whitening.

Snoek et al. [47] used the same architecture defined by Krizhevsky in the first tests with the CIFAR-10 dataset [17]. Considering the fact that deep networks have a significant number of hyperparameters (such as the number of layers, and the size of each layer), they developed a Bayesian Optimization procedure for tuning these hyperparameters. The network architecture is similar to the one used by Goodfellow, with two convolutional layers, but instead of the maxout neuron, Rectified Linear Units (RELUs) where used. Snoek et al. started training with the best hyperparameters obtained manually (by Krizhevsky), and used their method to fine-tune them. As a result, they were able to achieve 90.5% of accuracy on this task, compared to 82% of accuracy obtained by Krizhevsky. Again, the training dataset was augmented with translations and reflections to achieve this level of accuracy.

Ciresan et al. [18] proposed a method for image classification relying on multiple deep neural networks trained on the same data, but with different preprocessing techniques. The networks are trained separately, and then the results are combined, by averaging the outputs of the different networks. The architecture of the networks consisted of four convolutional layers, followed by a fully-connected layer, and a softmax layer. Training followed this procedure: At first, all images are preprocessed using multiple techniques, obtaining 5 different versions of each image - they used standard image processing techniques such as Histogram equalization, and Adaptive Histogram equalization. At the beginning of each epoch, each image in the dataset is randomly translated, scaled and rotated (i.e. the dataset is augmented). This updated dataset is then used to train the networks. During test, the images are pre-processed with the same techniques, and the results are combined by averaging the outputs of all networks. With this architecture, an accuracy of 88.79% was obtained.

Zeiler and Fergus [48] propose a regularization method for convolutional networks,

called stochastic pooling. The most common pooling strategy, max-pooling, works by selecting only the largest value of the pooling window. In the proposed method, a probability is assigned to each element in the window, where the larger values within the window are given higher probabilities. One of the values is then stochastically selected using these probabilities. At test time, the values of the window are averaged in a probabilistic form, by multiplying the values by their probability within the window. The network architecture contained three convolutional layers, each followed by stochastic pooling, and a local response normalization layer (which normalizes the pooling outputs at each location over a subset of neighboring feature maps). Lastly, a single fully-connected softmax layer is used to obtain the model predictions. With this architecture, an accuracy of 84.87% was obtained.

Hinton et al. [46] introduced a model regularization technique called dropout. The basic idea for dropout is that for each example (or mini-batch) of training, some of the neurons are deactivated (i.e. they are not used in the forward/back-propagation phases). In practice this is equivalent on training an ensemble of networks containing the set of all possible network configurations (i.e. all possible networks obtained by deactivating a given percentage of the neurons in each layer). At test time, the full network is used, which is equivalent to running the input in all possible network configurations, and averaging their result. The model for the CIFAR-10 dataset contained three convolutional layers, each followed by max-pooling and Local Response Normalization. A locally-connected layer is used after the convolutional layers, and a 50% dropout is used in this layer. The last layer is a softmax layer, which produces the model outputs. With this architecture, an accuracy of 84.40% was obtained.

3.1.1 Summary of the CIFAR-10 top results

Table 3.1 provides a summary of the papers reviewed above. The most important similarities among the models are the following:

1. All models used convolutional neural networks

2. No models used unsupervised pre-training

3. Best results used data augmentation (translation, rotation, scaling)

It is worth noting that none of top five results used unsupervised pre-training, in spite of the fact that such models, using RBMs and autoenconders, were fundamental for obtaining early successful results with deep learning. We can also see that the best results used techniques that expand (augment) the original datasets, such as translations and rotations.

Accuracy	**Algorithm**	**Preprocessing**	**Data Augmentation?**	**Pre-training?**	**Architecture**
90.65% [45]	Deep Convolutional Neural Network with Maxout	- Global contrast normalization - ZCA whitening	Yes: - Image translations - Horizontal Reflections	No	CNN with: - Convolutional maxout layers with max-pooling (x3) - Fully connected maxout layer - Softmax layer
90.50% [47]	Deep Convolutional Neural Network	Mean normalization	Yes: - Image translations - Horizontal Reflections	No	CNN with: - Convolutional layer followed by max-pooling and local contrast normalization (x2) - Two locally connected layers - Softmax layer
88.79% [18]	MCDNN (Multi-column Deep Convolutional Neural Network)	Image processing: - Image Adjustment - Histogram equalization - Adaptive Histogram Equalization - Contrast Normalization	Yes - Rotation $\pm 5^{\circ}$ - Scaling $\pm 15\%$ - Translation $\pm 15\%$	No	Several CNNs trained separately, and averaged in a MCDNN. CNNs are trained on data pre-processed using different techniques. - Used large number of wide layers (6 to 10 layers with hundreds of maps) - Used convolutional layers, with max-pooling
84.87% [48]	Deep Convolutional Neural Network	Mean normalization	No	No	CNN with: - Convolutional layer followed by stochastic pooling and local response normalization. (x3) - Softmax layer
84.40% [46]	Deep Convolutional Neural Network with Dropout	Mean normalization	No	No	CNN with: - Convolutional layers followed by pooling and local response normalization.(x3) - One locally-connected layer (where dropout of 50% is applied) - Softmax layer

Table 3.1: Comparison of top published results on the CIFAR-10 dataset

CHAPTER 4

METHODOLOGY

In this Chapter we propose a methodology to train Convolutional Neural Networks on texture classification problems. We start with a general definition on the learning process, and introduce the texture datasets that we use to evaluate the methodology. We then present our method for training the networks on texture problems, and the method we use to transfer learning between tasks.

From a high-level, the process to train and evaluate the models follows the standard method for pattern recognition problems. The objective is to use a machine learning algorithm to learn a classification model, using a training dataset. We can then use this model to classify new samples, with the expectation that the patterns learned by the model in the training set generalize for new data. This process is illustrated in Figure 4.1.

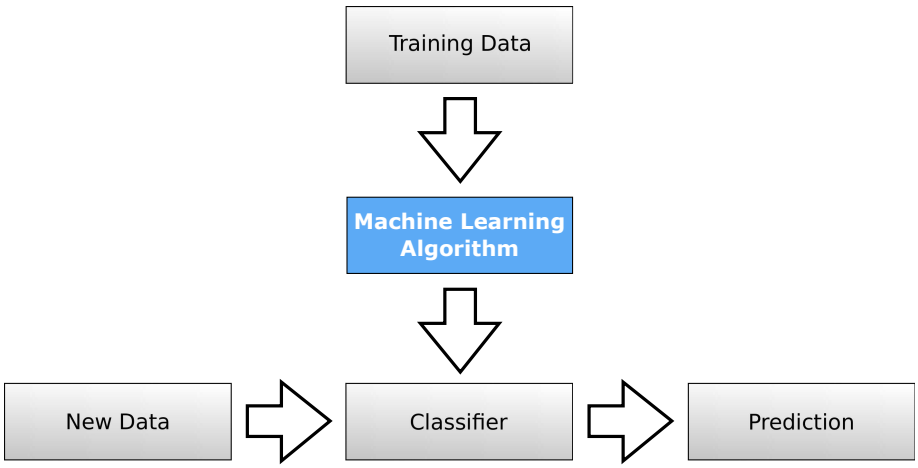

Figure 4.1: An overview of the Pattern Recognition process.

To evaluate the models, we use a held-out testing set to calculate the accuracy of the model, to verify how the model performs on unseen data:

$$\text{Accuracy} = \frac{\#\text{ correct predictions}}{\#\text{ samples in the testing set}} \tag{4.1}$$

For each dataset, the best architectures are validated using 3-fold cross-validation, that

is, the dataset is split three times (folds) into training, validation and testing. For each fold, a model is trained using the training and validation sets, and tested in the testing set. We then report the mean and standard deviation of the accuracy and compare them with the state-of-the-art in each dataset.

4.1 Texture datasets

A total of six texture datasets were selected to evaluate the method. These datasets were selected for two main reasons: they represent problems in different domains, and each dataset contain different challenges for pattern recognition. Below is a description of the selected datasets, with the different challenges that they pose. Examples of these datasets can be found in Appendix A

4.1.1 Forest Species datasets

The first dataset contains macroscopic images for forest species recognition: pictures of cross-section surfaces of the trees, obtained using a regular digital camera. This dataset consists in 41 classes, containing high-resolution (3264 x 2448) images for each class. The procedure used to collect the images, and details on the initial dataset (that contained 11 classes at the time) can be found in [49], and the full dataset in [50].

The second dataset contains microscopic images of forest species, obtained using a laboratory procedure. This dataset consists of 112 species, containing 20 images of resolution 1024x768 for each class. Details on the dataset, including the procedure used to collect the images can be found in [51]. Examples of this dataset are presented in Figure A.2. It is worth noting that the colors on the images are not natural from the forest species, but a result of the laboratory procedure to produce contrast on the microscopic images. Therefore, the colors are not used for training the classifiers.

The main challenge on the two forest species datasets is the image size. Most successful deep network models rely on small image sizes (e.g. 64x64), and these datasets contain images that are much larger.

4.1.2 Writer identification

We consider two writer identification datasets. The first is the Brazilian Forensic Letter Database (BFL), containing 945 images from 315 writers (3 images per writer)[52]. Hanusiak et al. [53] introduced a method to create textures from this type of image, transforming it into a texture classification problem. This method was later explored in depth by Bertolini [8] in two datasets: The Brazilian Forensic Letter Database, and the IAM Database. The IAM Database was presented by Marti and Bunke[54] for offline handwritten recognition tasks. The dataset includes scanned handwritten forms produced by approximately 650 different writers. Samples of these datasets, and their associated texture can be found in Figures A.4 and A.5. To allow direct comparison with published results on these datasets, we use the same subsets of the data as Bertolini [8]. In particular, we use 115 writers from the BFL dataset, and 240 writers from the IAM dataset. This large number of classes is the main challenge in these datasets.

4.1.3 Music genre classification

The Latin Music Dataset, introduced by Silla et al. [55] contains 3227 songs from 10 different Latin genres, and it was primarily built for the task of automatic music genre classification. Costa et al. [56] introduced a novel approach for this task, using spectrograms: a visual representation of the songs. With this approach, a new dataset was constructed, with the images (spectrograms) of the songs, enabling the usage of classic texture classification techniques for this task.

The music genre dataset contains a property that distinguishes it from the other datasets: on the other datasets, the textures are more homogeneous, in the sense that patches from different parts of the image have similar characteristics. For this dataset, however, there are differences in both axis: The music change its structure over time (X axis), and different patterns are expected on the frequency domain (Y axis). This suggest that convolutions can be less effective in this dataset, as patterns that are useful for one part of the image may not be useful for other parts. The challenge is to test if convolutions obtain good results in spite of these differences, or adapt the methodology to use a zoning

division, as described in the work by Costa et al. [56] and illustrated in figure 4.2.

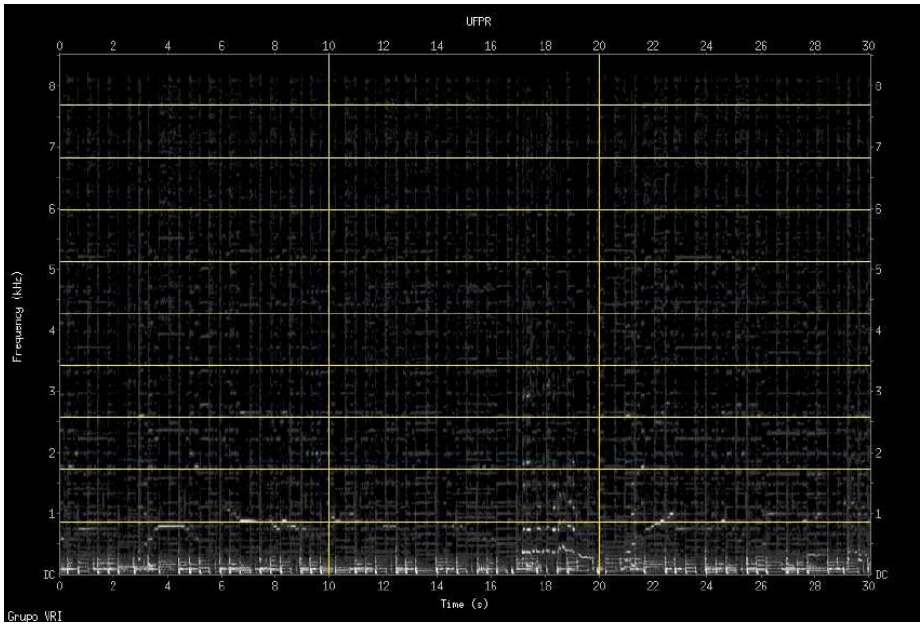

Figure 4.2: The zoning methodology used by Costa [56].

4.1.4 Brodatz texture classification

The Brodatz album is a classical texture database, dating back to 1966, and it is widely used for texture analysis. [57]. This dataset is composed of 112 textures, with a single 640x640 image per each texture. In order to standardize the usage of this dataset for texture classification, Valkealahti [58] introduced the Brodatz-32 dataset, a subset of 32 textures from the Brodatz album, with 64 images per class (64x64 pixels in size), containing patches of the original images, together with rotated and scaled versions of them (see Figure A.6).

The challenge with the Brodatz dataset is the lower number of samples per image. In the original Brodatz dataset, only a single image per texture is available (640x640). Since it is common for Convolutional Networks to have large number of parameters, this type of network usually require large datasets to be able to learn the patterns from the data.

4.1.5 Summary of the datasets

Table 4.1 summarizes the properties of the datasets used in this research, showing the different challenges (in terms of number of classes, database size, etc.) as mentioned in the previous sections.

The last column of the table counts the number of bytes used to represent the images in a bitmap format (i.e. 1 byte per pixel for grayscale images, 3 bytes per pixel for color images), to give a sense on the amount of information available for the classifier in each dataset.

Dataset	**Num. Classes**	**Num. Samples per Class**	**Total Num. of Samples**	**Image size**	**Number of bytes**
Forest species (Macroscopic)	41	37 ∼ 99	2942	3264 x 2448 (color)	∼65.7 GB
Forest species (Microscopic)	112	20	2240	1024 x 768	∼1.6 GB
Music Genre Classification	10	90	900	800 x 513	∼352 MB
Write identification (BFL)	115	27	3105	256 x 256	∼194 MB
Write identification (IAM)	240	18	4320	128 x 256	∼135 MB
Brodatz-32 Texture classification	32	64	2048	64 x 64	∼8 MB

Table 4.1: Summary of the properties of the datasets

4.2 Training Method for CNNs on Texture Datasets

The proposed method for training CNNs on texture datasets is outlined below. The next sections describe the steps in further detail, and provide a rationale for the decisions.

1. Resize the images from the dataset
2. Split the dataset into training, validation and testing
3. Extract patches from the images

4. Train a convolutional neural network on the patches using the training and validation sets

5. Test the network on the test patches

6. Combine the patches to report results on the whole test images

4.2.1 Image resize and patch extraction

Most tasks that were successfully modeled with deep neural networks usually involve small inputs (e.g 32x32 pixels up to 108x108 pixels). Networks with larger input sizes contain more trainable weights requiring significant more computing power to train, and also requiring more data to prevent overfitting.

In the case of texture classification, it is common to have access to high-resolution texture images, and therefore we need to methods that can explore larger inputs. Instead of simply training larger networks, we explore the hypothesis that we can classify a texture image with only a small part of it, and train a network not on the full texture images, but on patches of the images. This assists in reducing the size of the input to the neural network, and also allows us to combine, for a given image, different predictions made using patches from different parts of the image.

Besides the size of the input to the neural network, another important aspect is the size of the filter (feature map) for the first convolutional layer. The first layer is responsible for the first level of feature extractors, which are closely related to local features in the image. Therefore, the filter size must be adequate for the dataset images (and vice-versa), in the sense that relevant visual cues should be present in image patches of the size of the filter. Considering this hypothesis, we first resize the images so that relevant visual cues are found within windows of fixed filter sizes. We consider different filter sizes for the first layer following the results from Coates et al. [59], that investigated the impact of filter sizes in classification. Coates et al. empirically demonstrated that the best filter sizes are between 5x5 and 8x8. The usage of larger filter sizes would require significantly larger amounts of data to improve accuracy.

Besides this intuitive approach for choosing the filter size and the factor to resize the images, we also explore a more systematic approach, considering both as hyperparameters of the network, and optimizing them.

4.2.2 CNN architecture and training

The architecture of the neural networks are based on the best results on the CIFAR dataset (as reviewed in Chapter 3). In particular, we use multiple convolutional layers (each followed by max-pooling layers), followed by multiple non-convolutional layers, ending with a softmax layer. This architecture is illustrated in Figure 4.3

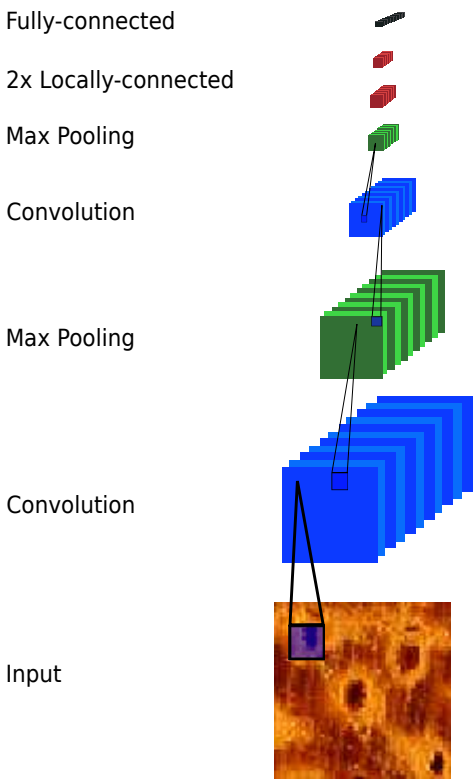

Figure 4.3: The Deep Convolutional Neural Network architecture.

This architecture consists of the following layers, with the following parameters:

1. *Input layer*: the parameters are dependent on the image resolution and the number of channels of the dataset;

2. *Two combinations of convolutional and pooling layers*: each convolutional layer has 64 filters, with a filter size defined for each problem, and stride set to 1. The pooling

layers consist of windows with size 3x3 and stride 2;

3. *Two locally-connected layers*: 32 filters of size 3x3 and stride 1;

4. *Fully-connected output layer*: dependent on the number of classes of the problem.

The network has a high number of hyperparameters, such as the number of layers, the number of neurons in each layer, and different parameters in each layer's configuration. In the present work we do not optimize all these hyperparameters. Instead, we started with network configurations that achieved state-of-the-art results on the CIFAR dataset, as described in Chapter 3, and performed tests in one of the texture datasets to select an architecture suitable for texture classification. We fixed the majority of the hyperparameters with this approach, we left the following hyperparameters for tuning:

- **Patch Size**: The size of the input layer in the CNN (cropped from the input image)
- **Filter Size**: The size of the filter in the first convolutional layer
- **Image size (Resize factor)**: The size of the image (before extracting its patches), resized from the original dataset. This is a parameter from our training strategy, not a parameter for the Convolutional Network. During initial tests, we found that this parameter is correlated with the Filter size, impacting the network's performance. For example, when the input image is large and does not contain relevant visual cues in a small area (e.g. 5x5 pixels) it requires larger filters to achieve good performance. To explore the impact of the image sizes together with the filter sizes, we consider both as hyperparameters to be optimized.

The training algorithm is similar to the Stochastic Gradient Descent algorithm (Algorithm 1) described in Chapter 2. The key difference is that the network is trained on random patches of the image - that is, for each epoch, a random patch is extracted for each image. We found that this strategy helps to prevent the model from overfitting the training set, while allowing training of a network with a large number of parameters. This procedure is defined in Algorithm 2 and illustrated in Figure 4.4.

Algorithm 2 Training with Random Patches

Require: dataset, patchsize, batch_size, learning_rate, momentum_factor

```
repeat
    dataset_epoch ← empty list
    for each image in dataset do
        Insert(dataset_epoch, Random_Image_Crop(image, patchsize))
    end for
    numBatches ← size(dataset) / batch_size
    for batch ← 0 to numBatches do
        dataset_batch ← dataset_epoch[batch * batch_size : (batch+1) * batch_size -1]
        model_state ← ForwardProp(model, dataset_batch.X)
        gradients ← BackProp(model_state, dataset_batch.Y)
        ApplyGradients(model, gradients, learning_rate, momentum_factor)
    end for
until Convergence_Criteria()
```

Here, **Random_Image_Crop** is a function that, given an image and a desired *patchSize*, returns a random patch of size (*patchSize* x *patchSize*). **ForwardProp** and **BackProp** are the forward-propagation and back-propagation phases of the CNN training, as defined in Chapter 2. **ApplyGradients** updates the weights using the gradients (derivatives), the learning rate and applying momentum. We considered different termination criteria, and good results were obtained by setting a maximum number of iterations without improvement in the error function.

We train the Convolutional Neural Networks on a Tesla C2050 GPU, using the cuda-convnet library[1].

4.2.3 Combining Patches for testing

During training, the patches extracted from the images are classified individually, to calculate the error function and the gradients. During test, the different predictions on each

[1] http://code.google.com/p/cuda-convnet/

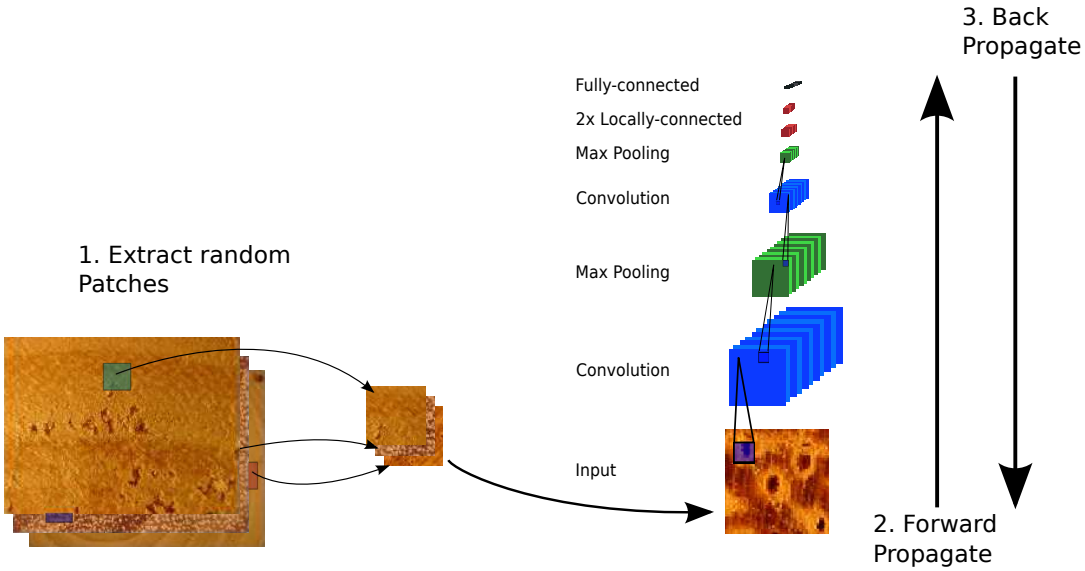

Figure 4.4: The training procedure using random patches

patch that compose an image need to be combined. For each patch, the model predicts the *a posteriori* probability of each class given the patch image. These probabilities are combined following the classifier combination strategies from Kittler et al. [39], reviewed in Chapter 2.

In the present work, we made the decision to use the set of all non-overlapping patches from the image during test (called here Grid Patches). For each image, we extract a list of patches, classify them all, and combine the probabilities from all patches of the image. This procedure is described in Algorithm 3 and illustrated in Figure 4.5.

Algorithm 3 Testing with Grid Patches

Require: dataset, patchsize, model

```
PatchesDataset ← empty list
for each image in dataset do
    Insert(PatchesDataset, ExtractGridPatches(image, patchSize))
end for
PatchProbabilities ← ForwardProp(model, PatchesDataset.X)
ImageProbabilities ← CombineProbabilities(PatchProbabilities)
Predictions ← argmax(ImageProbabilities)
ClassifiedCorrectly ← Count(Predictions = dataset.Y)
Accuracy ← ClassifiedCorrectly / Size(dataset)
```

Here, **ExtractGridPatches** is a function that divides an image in patches of size (*patchSize* x *patchSize*) and returns a list of patches. **ForwardProp** is the forward-propagation phase of the CNN; **CombineProbabilities** is a function that combines the probabilities from all patches of each image, using either the *Product Rule* or *Sum Rule* as defined in Chapter 2. The prediction for each sample is the class that has highest probability among all classes. We then calculate the Accuracy as the count of correctly classified samples, divided by the total number of samples in the testing set. When combining the probabilities, we experimented with both combination rules, and the *Sum Rule* consistently presented better results. Therefore this combination rule was used in our experiments.

4.3 Training Method for Transfer Learning

To explore the concept of transfer learning across different texture classification tasks, we use a procedure similar to the one used by Oquab et al. [41], but adapted to the training procedure above that considers random patches during training.

To recall, the objective of Transfer Learning is to improve the performance in a target task $\mathcal{T}_T$ with a source task $\mathcal{T}_S$ trained on a source domain $\mathcal{D}_S$. For example, we train a

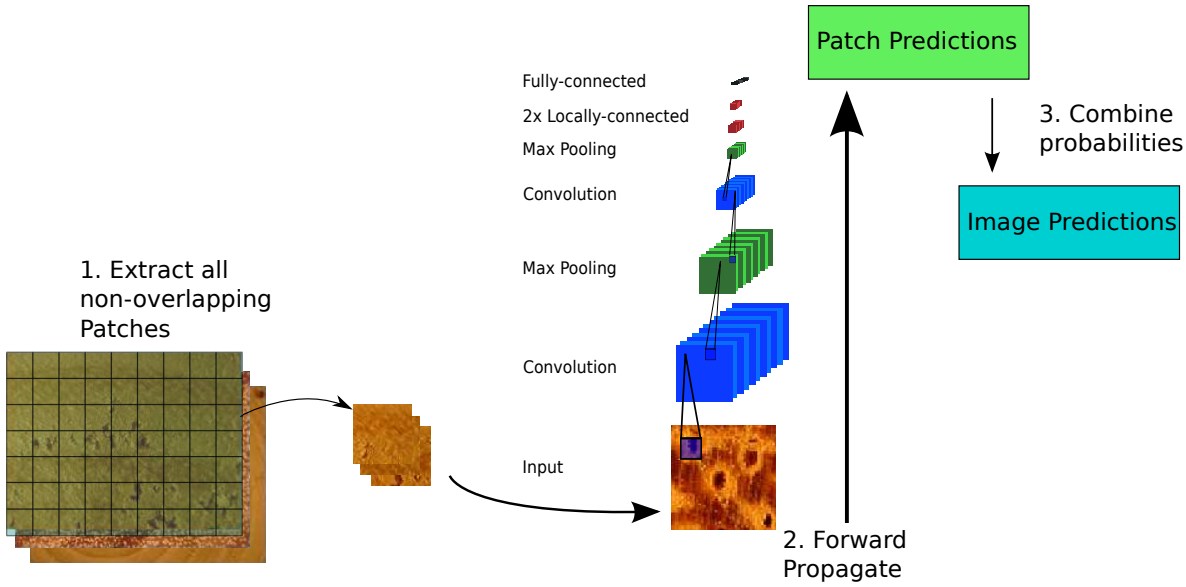

Figure 4.5: The testing procedure using non-overlapping patches

model on the IAM author identification task, and use this knowledge to improve a model trained for the BFL author identification task.

With this objective in mind, we follow these steps:

- Train a Convolutional Neural Network in the source task
- Use this network to obtain a new representation of the target task (project the data to another feature space)
- Use the new representation on the target task to train a new model

One interpretation for this procedure is to consider that the source task (e.g. learn a CNN model on the IAM dataset) learn feature extractors that are generic, to some extent, and that are useful for the target task. We use the CNN to extract a new representation for the target dataset, which is similar to using a feature extractor to the input, obtaining a new vector representation for each sample. When extracting the new representation, similar to Oquab et al. [41], we use the layers of the CNN (trained on the source task) up to the last layer before softmax. In contrast to their work, instead of training a neural network on the new representation, we experiment with two models: logistic regression and SVM (Support Vector Machines).

One challenge to apply this technique on our methodology is that, when training the CNN, we use patches of the original images, instead of the full image. This means that when we generate a new representation on the target dataset, we are generating new representations for patches of the target images. The challenge is how to select the patches from the target dataset for training. On the CNN training, we use one random patch per epoch, but this procedure does not work well with SVM, that require a static (fixed) dataset. To address this issue, for each image in the target dataset, we extract the set of all non-overlapping patches (Grid Patches). This fixed dataset is then used for training. On the test phase, we follow the same approach described above: extract the grid patches of the dataset, and later combine the results of all patches for each image. The algorithm for learning the new model is described in Algorithm 4 and illustrated in Figure 4.6.

Algorithm 4 Transfer Learning - training

Require: $\text{dataset\_train}_{\text{source}}$, $\text{dataset\_train}_{\text{target}}$, $\text{dataset\_test}_{\text{target}}$, patchSize

$\text{model}_{\text{source}} \leftarrow$ **Train_With_Random_Patches**($\text{dataset\_train}_{\text{source}}$, patchSize)

$\text{Patches\_train}_{\text{target}} \leftarrow$ *empty list*

for each image in $\text{dataset\_train}_{\text{target}}$ **do**

  Insert($\text{Patches\_train}_{\text{target}}$, **ExtractGridPatches**(image, patchSize))

end for

$\text{NewDataset\_train}_{\text{target}} \leftarrow$ **GetNewRepresentation**($\text{model}_{\text{source}}$, $\text{Patches\_train}_{\text{target}}$)

$\text{Model}_{\text{target}} \leftarrow$ **TrainModel**($\text{NewDataset\_train}_{\text{target}}$)

Here, **Train_With_Random_Patches** is the training procedure described in Algorithm 2; **ExtractGridPatches** is a function to extract all non-overlapping patches from a image; **GetNewRepresentation** is a function that runs the Forward-propagation phase of the CNN up to the last layer before Softmax, and returns the activations of the neurons on this layer. **TrainModel** is a function that trains a classifier using the given dataset. In our experiments we used a simple model (Logistic Regression) and Support Vector Machines (SVM).

The test procedure using Transfer Learning is also adapted to the fact that we use

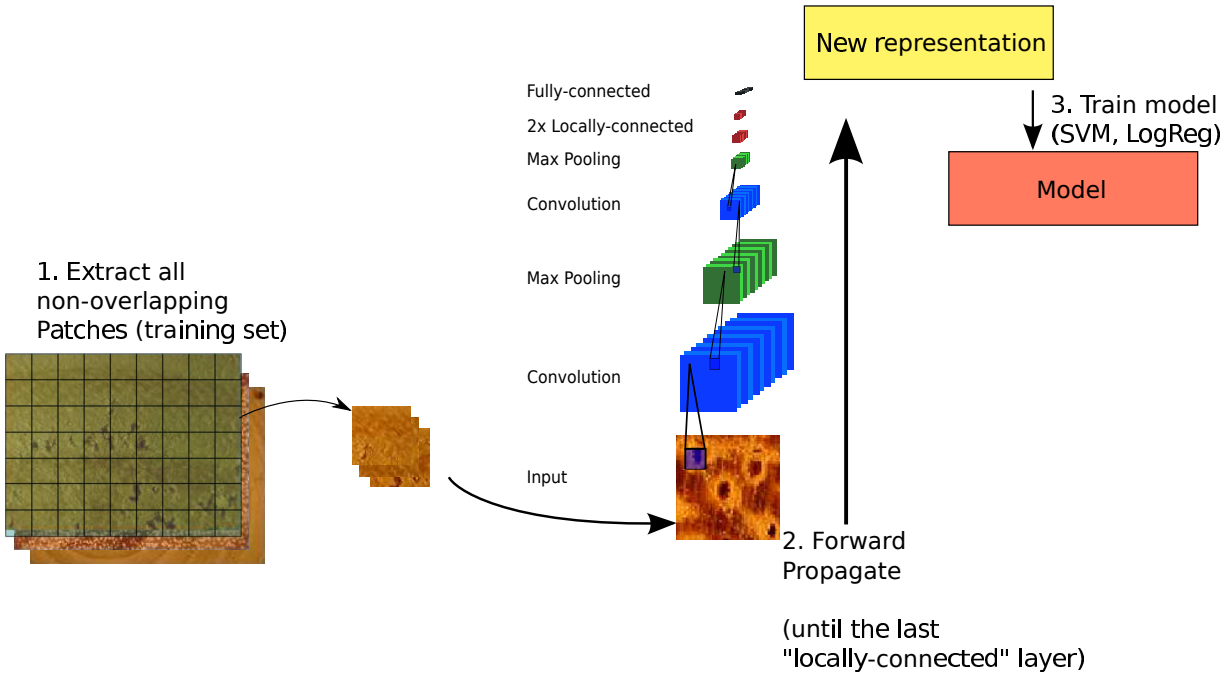

Figure 4.6: The training procedure for transfer learning

patches of the images on the CNN model. We extract the grid patches of the target dataset, use the model trained on the source task to generate the new representation, and use the model trained using algorithm 4 to generate the predictions for each patch of the image. Afterwards, we combine the results of the patches and report the accuracy. This procedure is described in Algorithm 5 and illustrated in Figure 4.7.

Algorithm 5 Transfer Learning - test

Require: $\text{model}_{\text{source}}$, $\text{model}_{\text{target}}$, $\text{dataset\_test}_{\text{target}}$, patchSize

$\text{Patches\_test}_{\text{target}} \leftarrow$ *empty list*

for each image in $\text{dataset\_test}_{\text{target}}$ **do**

$\text{Insert}(\text{Patches\_test}_{\text{target}}, \textbf{ExtractGridPatches}(\text{image}, \text{patchSize}))$

end for

$\text{NewDataset\_test}_{\text{target}} \leftarrow \textbf{GetNewRepresentation}(\text{model}_{\text{source}}, \text{Patches\_test}_{\text{target}})$

$\text{PatchProbabilities}_{\text{target}} \leftarrow \textbf{GetModelPredictions}(\text{model}_{\text{target}}, \text{NewDataset\_test}_{\text{target}})$

$\text{ImageProbabilities} \leftarrow \textbf{CombineProbabilities}(\text{PatchProbabilities})$

$\text{Predictions} \leftarrow \textbf{argmax}(\text{ImageProbabilities})$

$\text{ClassifiedCorrectly} \leftarrow \text{Count}(\text{Predictions} = \text{dataset\_test}_{\text{target}}.\text{Y})$

$\text{Accuracy} \leftarrow \text{ClassifiedCorrectly} \;/\; \text{Size}(\text{dataset})$

Here, **GetModelPredictions** is a function on the target model (Logistic Regression or SVM) that returns the probabilities of each class for each training example (each patch). The remainder of the procedure follows the same steps as algorithm 3: the probabilities of patches of each image are combined, and the accuracy is reported as the number of correctly predicted samples divided by the number of samples in the testing set.

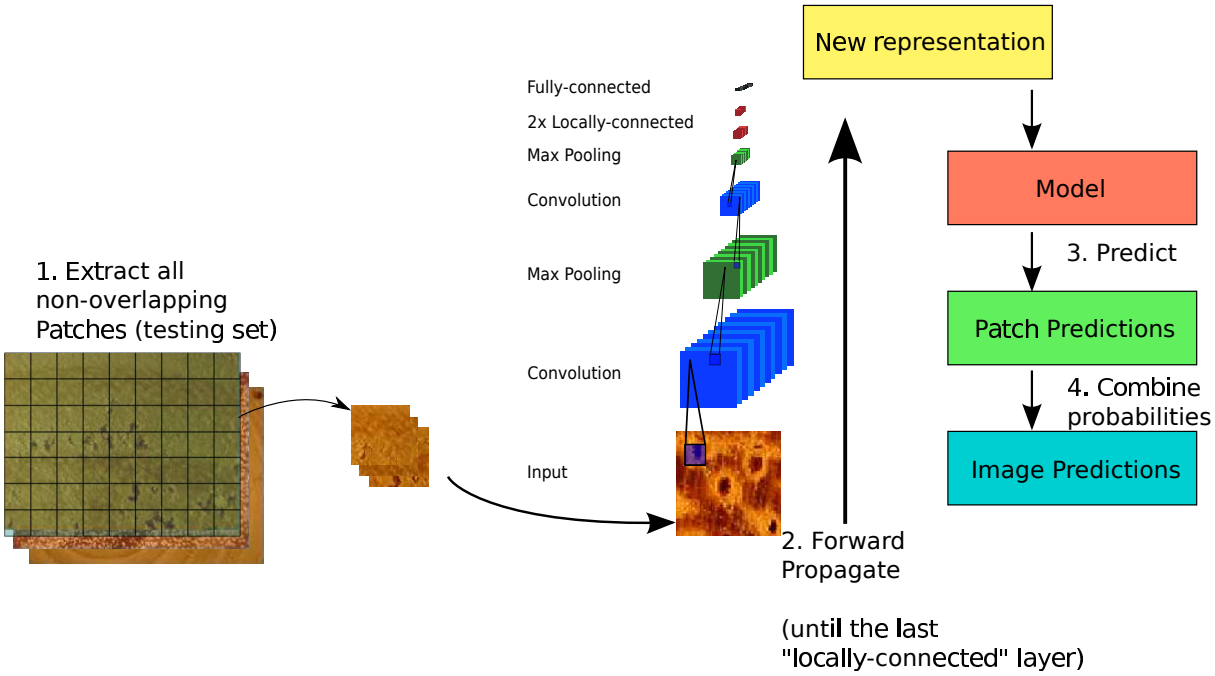

Figure 4.7: The testing procedure for transfer learning

CHAPTER 5

EXPERIMENTAL RESULTS

We now present the results from experiments performed with the proposed methodology. We start with the experiments to train a Convolutional Neural Network on each of the texture datasets, followed by the experiments with Transfer Learning.

5.1 Forest species recognition tasks

The first experiments were conducted with the datasets for forest species classification. The two datasets have a large number of images with high resolution, and we use the methodology described in Chapter 4 to handle this challenge (large image sizes).

For both datasets, we first reduced the input size by resizing the images. The objective was to ensure that discriminative visual cues could be found in small regions of the images, enabling the model to learn discriminative patterns in the first convolutional layers.

For the Macroscopic images, we noticed that although the images are large (3264 x 2448), they are not very sharp - small regions such as 5x5 or 10x10 are blurred, and do not have discriminative features. Based on this analysis we selected to test the following image sizes: 326 x 244 (10% of the original) and 652 x 488 (20% of the original).

For the microscopic images, the images are smaller (1024 x 768), and they are already crisp. For this dataset, however, we noticed that some textures are not homogeneous - for example, some samples contain large holes, that could only be captured by either using much large filters, or by resizing the image to smaller sizes. We explore this idea by training models with the following image sizes: 307 x 230 (30%), 512 x 384 (50%), 716 x 537 (70%) and 1024 x 768 (100%).

For each dataset and for each configuration of the hyperparameters, we trained one Convolutional Neural Network following the methodology from Chapter 4 and calculated the accuracy. For the dataset with Macroscopic images, training a model took about

1.2 hours, and for the dataset with Microscopic images, training took close to 3h. The following sections review the results.

5.1.1 Classification rates

Figure 5.1 summarizes the error rates (number of misclassified samples divided by the total number of samples) on the Macroscopic dataset, for each CNN trained with a particular set of hyperparameters. The table on the left summarizes the results of the networks trained on images resized to 10% (326 x 244), and the table on the right summarizes the results of the networks trained on images resized to 20% (652 x 488). For each table, we have one entry for each combination of **Patch Size** and **Filter Size** (size of the filter on the first convolutional layer). The color of the cell indicates the error - lower error rates (better models) are displayed in lighter colors.

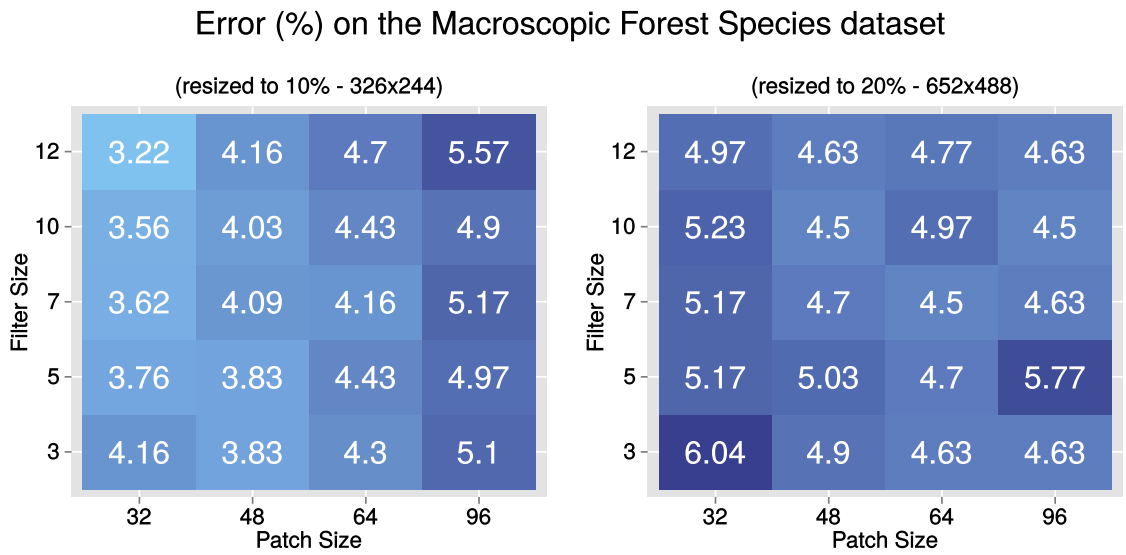

Figure 5.1: Error rates on the Forest Species dataset with Macroscopic images, for CNNs trained with different hyperparameters.

The model with lowest error rate was the model trained on the dataset resized to 10% of the original size, using the smallest patch (32x32) and the largest filter size (12x12). This model obtained an error rate of 3.22% (or, equivalently, an accuracy of 96.78%). It is worth noting that, during test, we extract the set of non-overlapping patches from the images and combine the results. This means that using large patch sizes implies in

dividing an image in less patches. For example, for patches of size 32x32, the image is divided in 70 patches, while for the 96x96 patches, the image is divided in 6 patches.

Figure 5.2 summarizes the error rates on the Microscopic dataset, for each CNN trained with a particular set of hyperparameters:

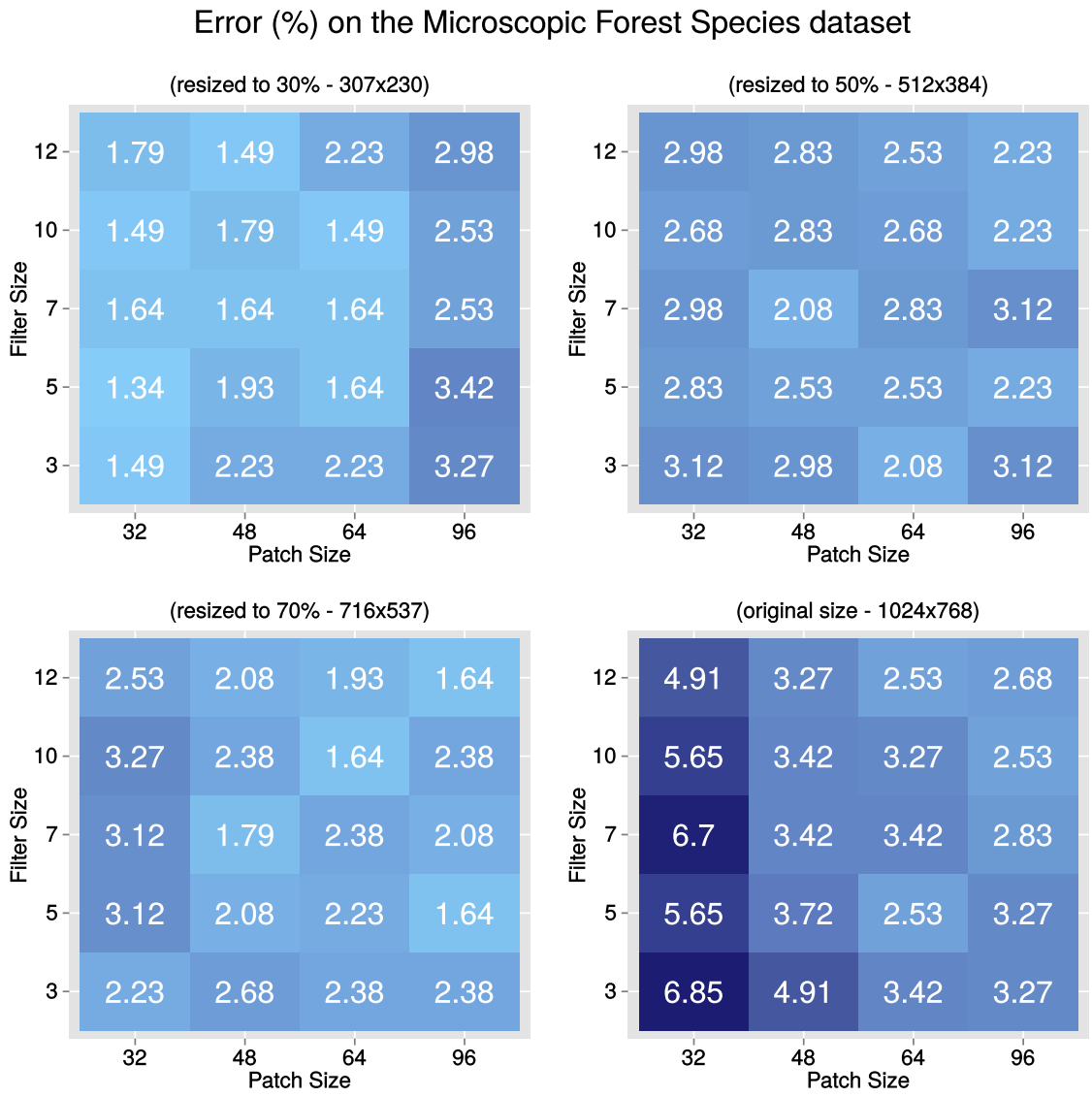

Figure 5.2: Error rates on the Forest Species dataset with Microscopic images, for CNNs trained with different hyperparameters.

For this dataset, the model with lowest error rate was trained on the dataset with the images resized to 30% of the original size, with Patch Size 32x32 and filter size 5x5. We noticed that the models trained on the images with original size performed poorly compared to models trained on reduced images. Even though the visual analysis of the original image suggested that small regions already contained relevant visual cues, these

may not be useful (discriminative) features for the model, supporting the argument that it is better to consider the image size as a hyperparameter and run models with different image sizes.

Figure 5.3 shows the predictions of a model trained on the Macroscopic images. A total of eight random patches from the testing set are displayed, with the top 4 classes predicted by the model (that is, the classes with higher probability according to the model). In this figure, the sizes of the horizontal bars are the probability assigned for the sample to a particular class, and the bar in the color red is the correct label (also displayed below the image). For ease of understanding, the classes were numbered (from 0 to 40) instead of using the names of the trees. We can see that the model predicts with high confidence the majority of the samples.

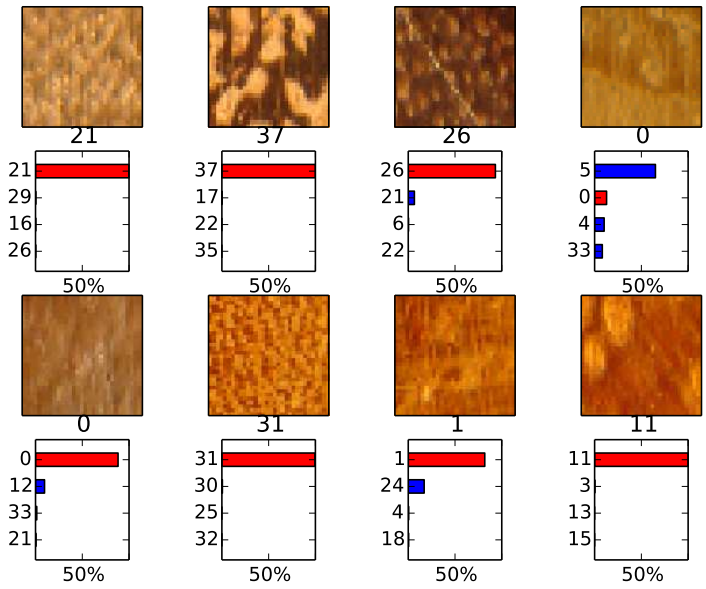

Figure 5.3: Random predictions for patches on the Testing set (Macroscopic images)

Figure 5.4 displays the predictions of a model trained on the Microscopic images. Similarly with the case for the Macroscopic dataset, we see that the model often provides high confidence on the probabilities. Unfortunately, this is the case even when the model is incorrect on the prediction (for example the image of class 92, misclassified as class 57).

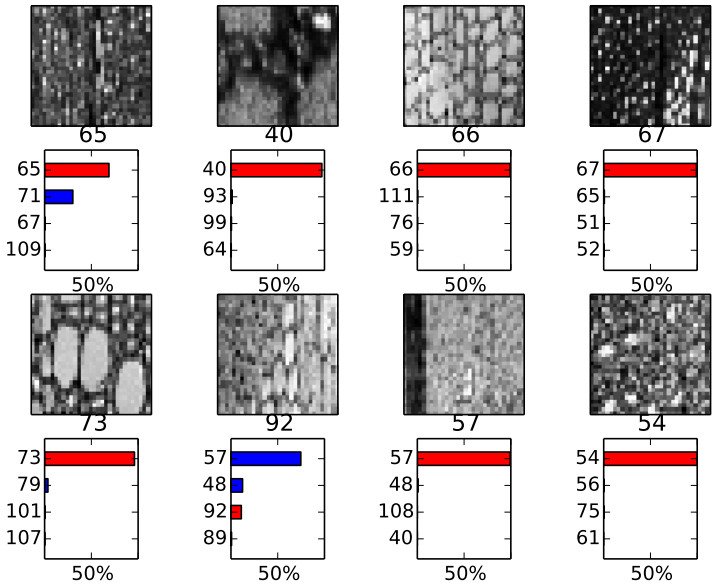

Figure 5.4: Random predictions for patches on the Testing set (Microscopic images)

5.1.2 Feature Learning

As discussed in Chapter 1, one of the advantages of using deep learning techniques is not requiring the design of feature extractors, but instead let the model learn them. It is possible to visualize the feature detectors that model learn on the first convolutional layer, considering the weights on the learned filters (feature maps). Figure 5.5 displays the filters that were learned in the first convolutional layer for the networks trained on the macroscopic images dataset. In this figure, we consider the networks trained on the images resized to 10% of the original (326 x 244), with small patch sizes (32x32) and large patch sizes (96x96). We can observe that in the majority of the cases the networks learn interesting feature detectors, some similar to edge detectors, others capturing color changes, and other filters that look particular to this dataset (such as the ones that resemble small holes in the woods). We can also observe that larger filter sizes seem to work better (i.e. learn more interesting features) with large patch sizes. However, considering that the performance with large patches is worse (as seen in Figure 5.1) we can infer that although using larger patch sizes helps in classifying each patch, it does not compensate the fact that we have fewer patches to combine in the final image.

Figure 5.6 contains the features learned in the first convolutional layer for the network that presented best results on the Microscopic images dataset. The network was trained

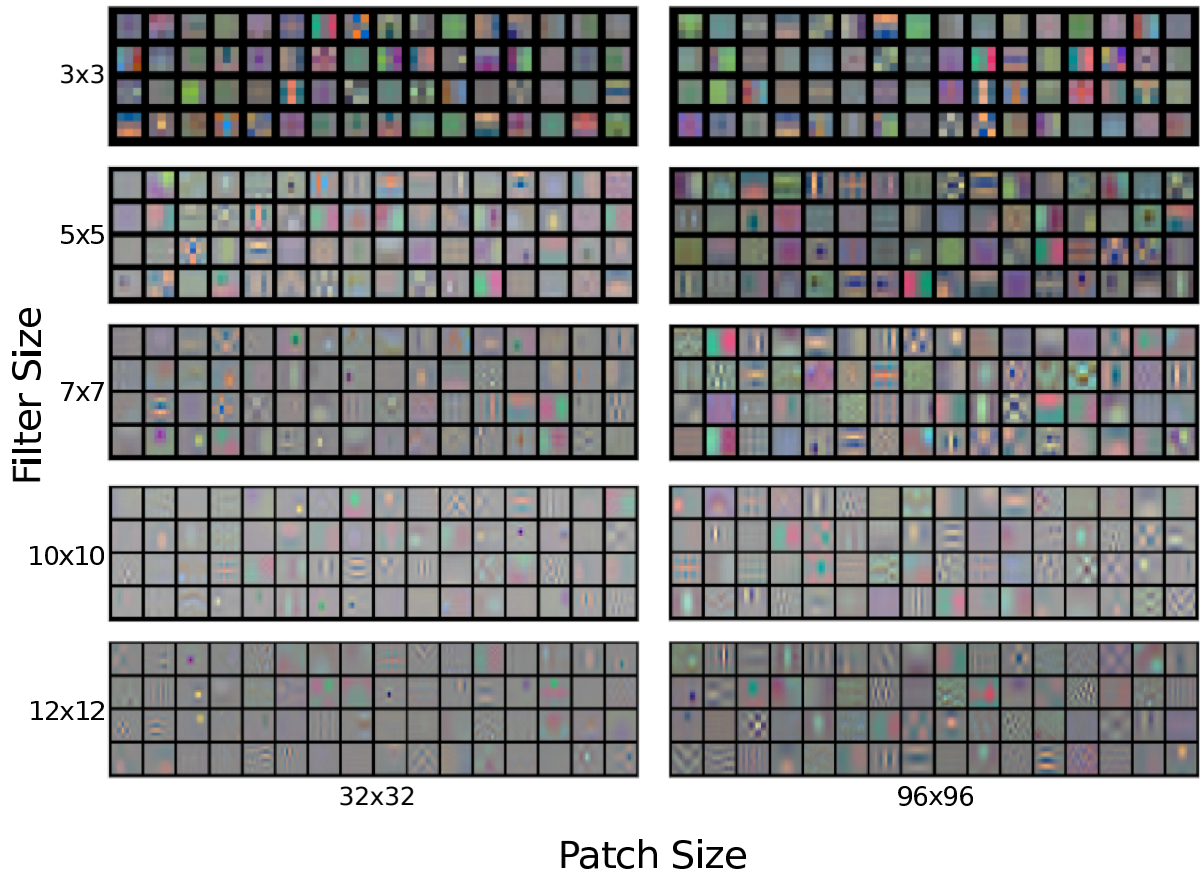

Figure 5.5: Filters learned by the first convolutional layers of models trained on the Macroscopic images dataset.

on images of size 308 x 230 (30% of the original), with filter size 5 and patch size 32.

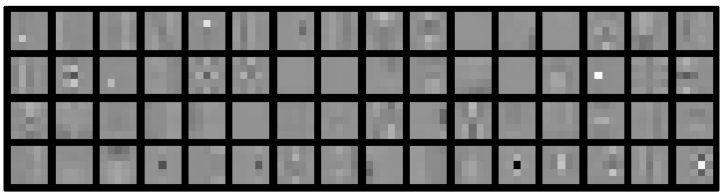

Figure 5.6: Filters learned by the first convolutional layer of a model trained on the Microscopic images dataset.

5.1.3 Comparison with the state of the art

The dataset with Macroscopic images has been analyzed and tested using texture classification techniques by Paula et al. in [50], [5] and [60]. The best results were achieved with a combination of multiple SVM classifiers trained with different texture feature descriptors: GLCM, LBP, CLBP and color-based features (color histograms).

Table 5.1 summarizes the result of the convolutional neural network trained on the macroscopic dataset, and compares it with the current state-of-the-art on this dataset. We can see that the convolutional neural network achieves state-of-the-art results compared with previous results with a single classifier, and reaches close to the best published result, that uses a combination of 6 different classifiers (trained with CLBP (x2), LBP, Gabor-filters, Fractals and Color-based features).

Table 5.1: Classification on the Macroscopic images dataset

Features and Algorithm	Accuracy
LBP (SVM) [60]	85.84%
Color-based features (SVM) [60]	87.53%
Gabor filters (SVM) [60]	87.66%
CLBP (SVM) [60]	96.22%
Multiple classifiers (SVM) [60]	**97.77%**
Proposed method (CNN)	96.24% (+- 0.27%)

On the Microscopic images dataset, the best published result is from Cavalin et al. [61]. Cavalin et al. trained SVM classifiers using GLCM, LBP and LPQ features. The best result was achieved by a combination of the LPQ and GLCM features, achieving 93.2% of accuracy in the 112-class problem.

Table 5.2 summarizes the result of the convolutional neural network trained on the microscopic dataset. The proposed model outperforms the best published results on this dataset by a large margin:

Table 5.2: Classification on the Microscopic images dataset

Features and Algorithm	Accuracy
LBP (SVM) [51]	86.00%
GLCM (SVM) [61]	80.70%
LBP (SVM) [61]	88.50%
LPQ (SVM) [61]	91.50%
LPQ + GLCM (SVM) [61]	93.20%
Proposed method (CNN)	**98.16%** (+- 0.37%)

5.2 Author Identification tasks

We now consider the experiments on the author identification tasks, for the BFL and the IAM datasets. These datasets contain a larger number of classes (115 for the BFL dataset, 240 for the IAM dataset), and therefore they are useful to evaluate how this methodology scales with the number of classes in the classification task.

To enable direct comparison with the results from Bertolini et al. [8], we use the images preprocessed by Bertolini as input (that is, the texture images, instead of the original letters), and the same number of classes. For the BFL dataset we used a subset with 115 classes, randomly selected from the original 315 writers. For each class, we have 27 texture images of size 256 x 256, which were generated from three original letters from the authors (9 textures generated for each letter). We split these 27 images into training, validation and testing sets, making sure that the textures from the same letter remain on the same set (i.e. 9 images from the same letter on each set). For the IAM dataset, we used a subset of 240 classes, randomly selected from the classes with two or more letters. For each class, we use 18 texture images of size 128x256, which were generated from the two original letters (9 textures for each letter). Again, we make sure that all the textures associated with the letter used for the testing set are not present in the training set.

For these datasets, the images are already reasonably small. Resizing the images to smaller sizes would reduce significantly the amount of patches that we can extract from them, and thus we tested only with the original image sizes. Another observation we made is that the images are consisted mostly of white background (pixels of intensity 255), with pen strokes in black on the foreground (pixel intensity very close to 0). Since these are the inputs to the neural network, one hypothesis is that we would obtain better results if the pen strokes, instead of the background, had values different than 0. We tested this hypothesis by training a network with the original textures, and a network with the textures with their color inverted. We observed a small performance increase using the textures with inverted color (white strokes on black background) and for the remaining of the tests we used this approach.

After these initial definitions, we followed our methodology to train Convolutional

Neural Network models on these datasets. We observed that these models took longer to converge than the models trained on the forest species datasets. Training a model on the IAM dataset took about 3.6 hours, and about 5.6 hours on the BFL dataset.

5.2.1 Classification rates

Similarly for the datasets above, we trained models on each dataset varying two hyperparameters (Patch size and Filter size). Figure 5.7 shows the error rate for models trained on the IAM dataset, with different hyperparameters:

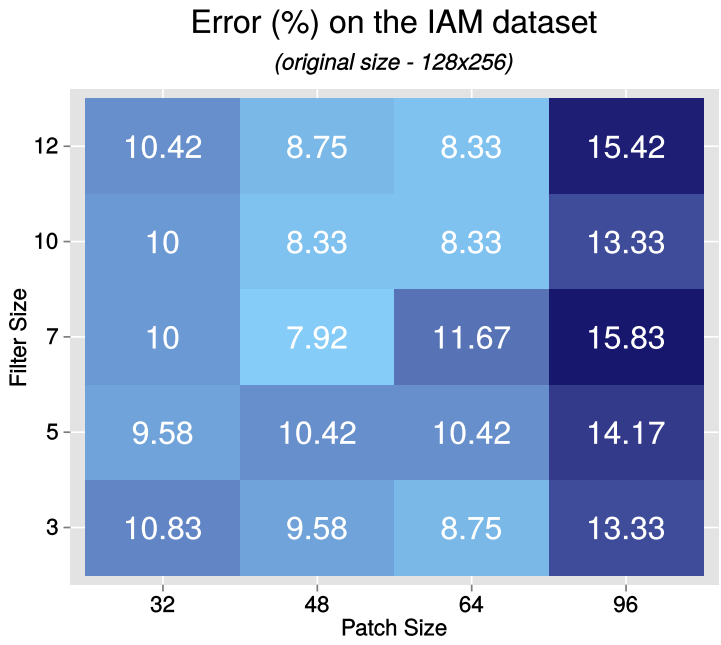

Figure 5.7: Error rates on the IAM dataset, for CNNs trained with different hyperparameters.

The best result was achieved by a model trained with Filter size 7x7 and Patch size 48x48, for an error rate of 7.92%. Similarly to the Macroscopic Forest Species dataset, we noticed that the models trained with larger patch sizes (96x96) performed poorly after the combination of all patches from the images, even though they performed well to classify the individual patches. This showed again that the increased accuracy in classifying each patch did not compensate the fact that fewer patches were available for combination in the later step.

Figure 5.8 shows the error rate for models trained on the BFL dataset, with different hyperparameters:

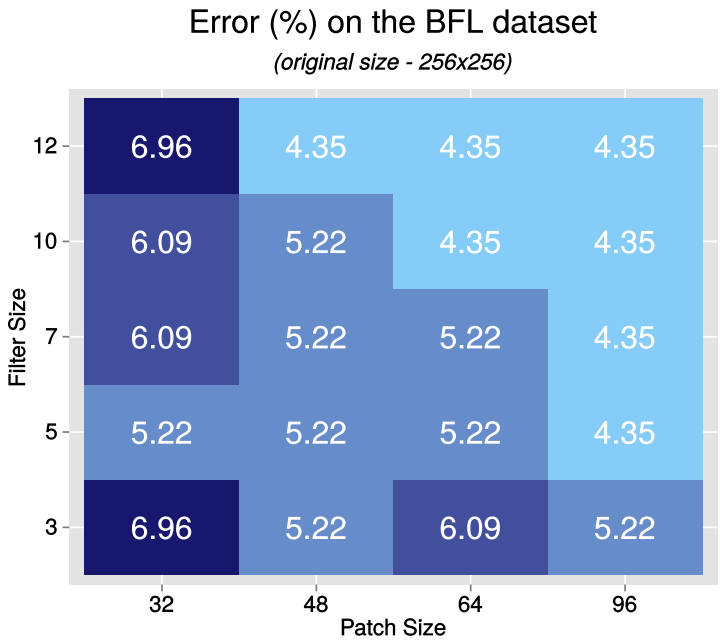

Figure 5.8: Error rates on the BFL dataset, for CNNs trained with different hyperparameters.

The best result was achieved by models trained with different hyperparameters, using large patch sizes and large filter sizes. It is interesting to notice that the hyperparameter search in the BFL dataset displayed results completely different from the IAM dataset (that performed better with smaller patches, and smaller filter sizes), in spite of using similar datasets.

Examples of classifications for the IAM dataset can be seen in Figure 5.9. This figure displays eight random patch predictions for the dataset. Since the names of the authors are not available, we associate a number to each one. We can see that the input for the neural network consists of a small set of pen strokes in each patch. In this dataset, we notice that the network makes more mistakes on the individual patches, and therefore the combination of patches in the images plays an important role in obtaining good results.

For the BFL dataset, since the tests with the hyperparameters presented equal results for multiple combinations of patch size and filter size, we selected one of the models for evaluating the predictions. Figure 5.10 shows eight random patches from the testing set

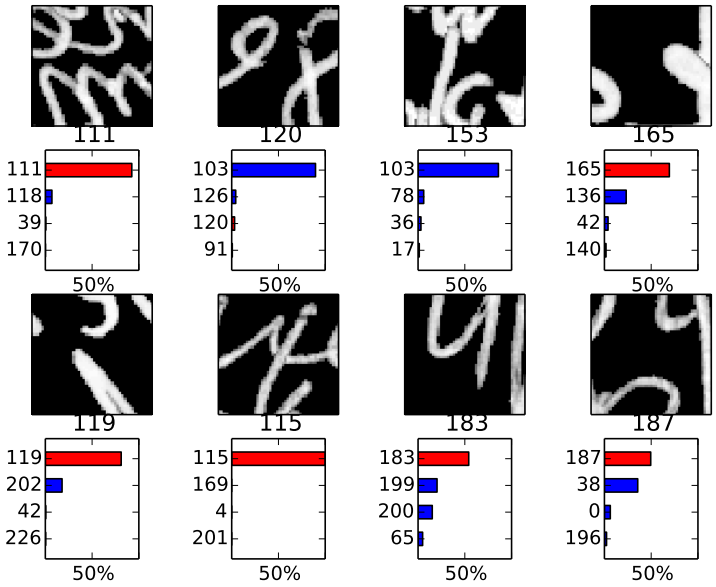

Figure 5.9: Random predictions for patches on the IAM Testing set

of the BFL dataset in the model with patch size 64x64 and filter size 10x10. Again we see the model making several mistakes when classifying the patches, but from the results after the combination of all patches for an author's letter we see that the combination of patches minimizes the number of errors.

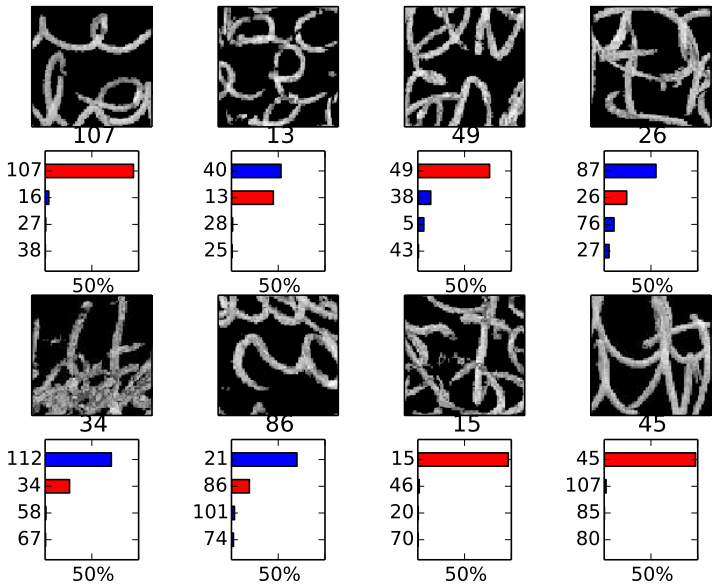

Figure 5.10: Random predictions for patches on the BFL Testing set

5.2.2 Feature Learning

Figures 5.11 and 5.12 shows the filters learned by the first convolutional layers in the IAM and BFL datasets respectively. We can see very similar feature detectors learned by the two networks, with several filters that learned how to capture small parts of a pen stroke: horizontal, vertical and diagonal straight lines, as well as some curved lines.

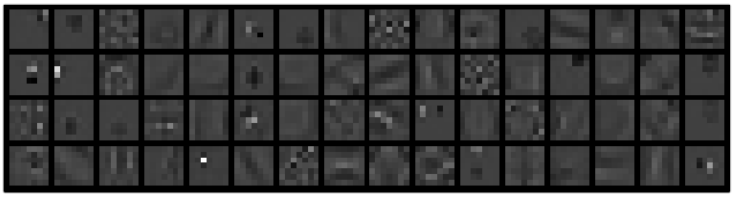

Figure 5.11: Filters learned by the first convolutional layer of a model trained on the IAM dataset.

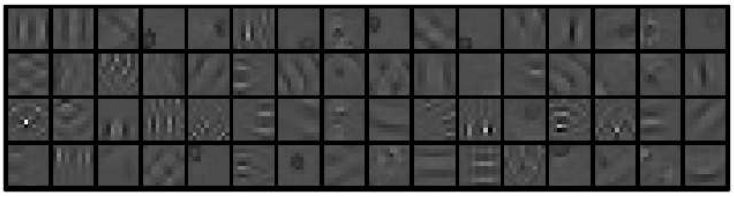

Figure 5.12: Filters learned by the first convolutional layer of a model trained on the BFL dataset.

5.2.3 Comparison with the state of the art

Table 5.3 compares the results above with the best published result on the IAM dataset. For this dataset, the best results were presented by Bertolini et al. [8]. We compare our results with the writer-dependent approach from Bertolini et al., as their results using a dissimilarity framework (a writer-independent approach) are not directly comparable. We can see that the proposed method outperforms the previous result on this dataset.

Table 5.3: Classification on the IAM dataset

Features and Algorithm	Accuracy
LPQ (SVM) [8]	88.30%
Proposed method (CNN)	**91.39%** (+- 0.51%)

Table 5.4 compares the results of the proposed method with the best published result on the BFL dataset. For this dataset, the best results were presented by Bertolini et al.

[8]. Again, we compare our proposed method with the writer-dependent approach from Bertolini et al. (i.e. without using dissimilarity). For this dataset, the proposed method with a CNN performs worse than the state-of-the-art.

Table 5.4: Classification on the BFL dataset

Features and Algorithm	Accuracy
LPQ (SVM) [8]	**98.26**%
Proposed method (CNN)	95.36% (+- 0.41%)

5.3 Music Genre classification task

This section describes the results on the Latin Music Dataset. For this experiment we use the dataset processed by Costa et al. [56] instead of the original song fragments, that is, we use the spectrograms generated from each sample as input to our classifier. These images present a challenge compared to the datasets used above, since these are not homogeneous textures: we observe that the textures have different patterns in different regions of the image, as we move in the X axis (time) or the Y axis (frequency) in the spectrogram. We applied the proposed method on this dataset, and the results were poor. Initial experiments achieve an accuracy of 54% on the testing set, which is a poor result for a classification task with only 10 classes. This result can be justified by the fact that our method does not consider the location of each patch during classification, and therefore it works best when the texture presents similar patterns across the image.

After these initial tests, we attempted the same zoning strategy as Costa et al. [56]. The approach is to partition the image in both axis (time and frequency), and train a classifier for each part. We split our image in three parts in the X axis (time) and in 10 parts in the Y axis (frequency), giving a total of 30 regions. For each region, we trained a Convolution Neural Network following the proposed methodology. During test, we split the images from the testing set into these 30 regions, obtain the predictions from each network, and combine the results of the 30 classifiers, following again the classifier combination strategies from Kittler et al. [39], reviewed in Chapter 2. Again, we obtained better results with the *Sum Rule* for combining the classifiers. Each of the 30 networks

took about 2 minutes to train, for a total of 1h of training time.

5.3.1 Classification rates

We performed experiments with different values of the hyperparameters Filter Size and Patch Size. Since we split the image in 30 regions, the input for each neural network is very small. Therefore, we limited our search on patch sizes smaller than these regions (patches of size 32x32 and 48x48). We also noticed that the original images were not very sharp. For this reason we decided to test both models with the original image size (800x513), and models trained on images resized to 60% of the original size (480 x 307). Figure 5.13 shows the results from these experiments:

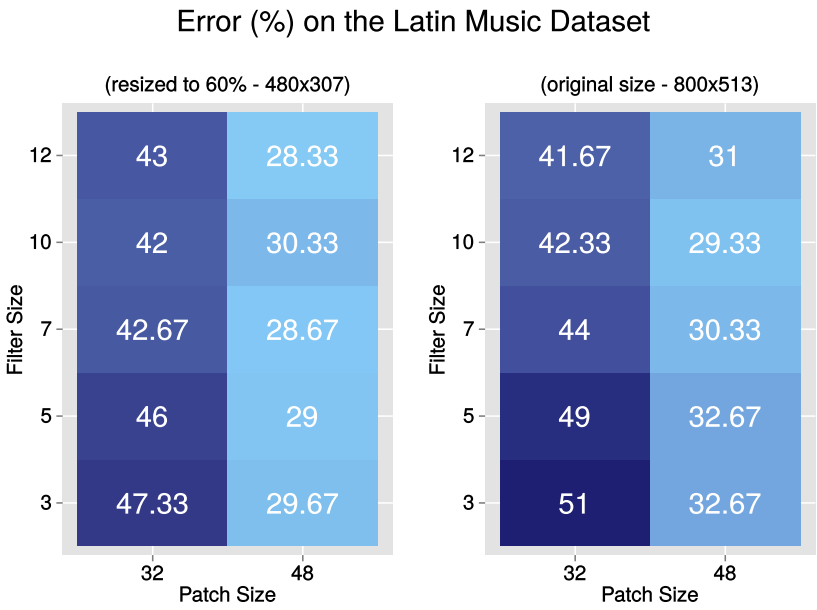

Figure 5.13: Error rates on the Latin Music Dataset, for CNNs trained with different hyperparameters.

We noticed similar results for different filter sizes, with the best result obtained by a network trained on images resized to 60% of the original size, and with Filter size 12x12 and Patch size 48x48. These results showed an improvement over the training a single CNN for the task, but with error rates that are still high for a 10-class classification task.

Figure 5.14 shows eight random predictions for patches on the test set. We selected the predictions of a model trained in one of the 30 divisions of the test images - here we

show the predictions on the region $(6, 1)$ - that is, the region corresponding to row 6 (on the Y axis) and column 1 (on the X axis). We can see that the model is not very reliable on its predictions, except on a few cases.

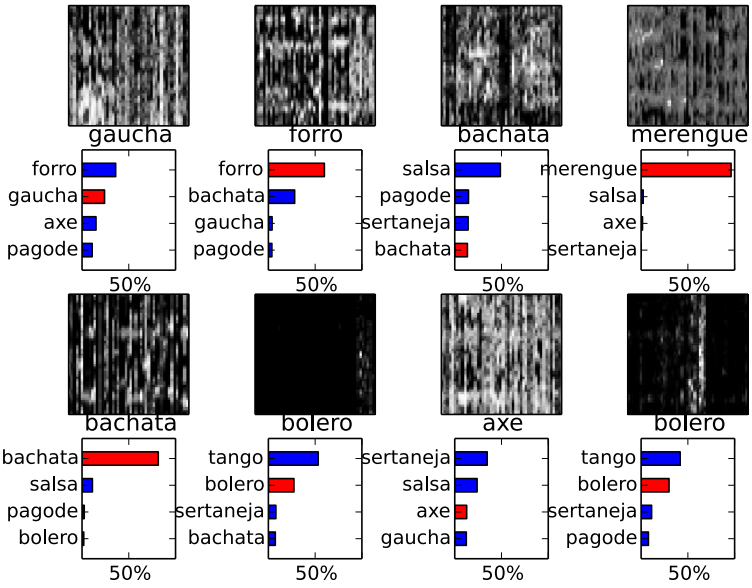

Figure 5.14: Random predictions for test patches on the Latin Music Dataset

5.3.2 Feature Learning

Figure 5.15 displays the filters learned by the first convolutional layer of the model trained in region $(6, 1)$. The model seems to learn the patterns present on the histogram, but from the experimental results we can infer that these patterns are not very discriminative for the task.

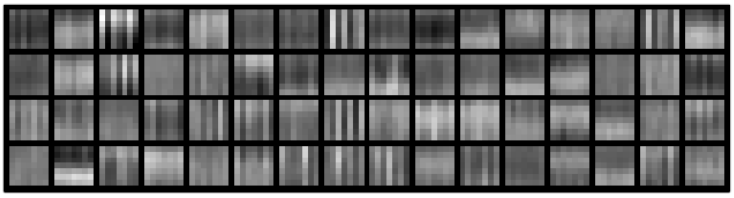

Figure 5.15: Filters learned by the first convolutional layer of a model trained on the Latin Music dataset.

5.3.3 Comparison with the state of the art

Table 5.5 compares the result of the proposed method with the best published results. For this dataset, Costa et al. used SVM classifiers with LBP (Local Binary Patterns) to obtain the best results. Using this type of classifier with zoning strategies, a classification accuracy of 82.33% was obtained. The accuracy with the proposed method did not match the state-of-the-art for this task. One potential reason for the poor performance is the fact that each CNN trained for this dataset has little data available (since we are dividing the images in 30 parts and training a network in each part) - analyzing the filters learned by the models, it seems that they were not able to learn discriminative features. It is also worth noting that, during the 3-fold validation, we identified a larger variance in the classification performance, compared to the CNNs in other tasks.

Table 5.5: Classification on the Latin Music dataset

Features and Algorithm	Accuracy
LPQ + Gabor Filters (SVM) [9]	80.78% (+- 0.77)
LBP (SVM) [56]	**82.33**% (+- 1.45)
Proposed method (CNN)	73.67% (+- 1.41%)

We now compare the errors committed by the proposed method (CNN) with errors made by the model from Costa et al. [9]). The objective is to identify if the models commit similar types of errors, or if they present different types of errors - suggesting that the two models offer complementary information.

Table 5.6 shows the confusion matrix of our model (the combination of CNNs trained in segments of the image). In this table, the rows contain the actual (true) labels, and the columns contain the predictions. Each cell contains the percentage of the samples of the actual class (row) that were predicted as a particular class (column). Table 5.7 contains the same type of information, for the results published by Costa et al. Comparing the two tables, we see that in most cases the types of errors are similar. In few cases the proposed method performs better - in the classification of class 9 (Tango) overall, for mistakes between class 0 (Axé) and class 6 (Pagode); mistakes between class 8 (Sertaneja) and class 4 (Gaúcha), among others. With this comparison, we expect that the combination

of the two types of models can bring a small improvement in the current state-of-the-art.

Table 5.6: Confusion Matrix on the Latin Music Dataset classification (%) - Our method

Class	(0)	(1)	(2)	(3)	(4)	(5)	(6)	(7)	(8)	(9)
(0) Axé	**67.78**	5.56	3.33	2.22	4.44	6.67	1.11	1.11	7.78	0.00
(1) Bachata	1.11	**92.22**	2.22	0.00	0.00	1.11	0.00	3.33	0.00	0.00
(2) Bolero	0.00	3.33	**85.56**	1.11	1.11	0.00	0.00	0.00	1.11	7.78
(3) Forró	1.11	1.11	7.78	**74.44**	4.44	0.00	1.11	4.44	5.56	0.00
(4) Gaúcha	15.56	1.11	12.22	8.89	**51.11**	2.22	0.00	4.44	4.44	0.00
(5) Merengue	0.00	5.56	1.11	0.00	0.00	**93.33**	0.00	0.00	0.00	0.00
(6) Pagode	4.44	5.56	21.11	4.44	4.44	1.11	**45.56**	8.89	4.44	0.00
(7) Salsa	3.33	2.22	5.56	0.00	0.00	3.33	1.11	**81.11**	3.33	0.00
(8) Sertaneja	12.22	3.33	11.11	10.00	3.33	3.33	1.11	2.22	**53.33**	0.00
(9) Tango	0.00	0.00	7.78	0.00	0.00	0.00	0.00	0.00	0.00	**92.22**

Table 5.7: Confusion Matrix on the Latin Music Dataset classification (%) - Costa et al.[9]

Class	(0)	(1)	(2)	(3)	(4)	(5)	(6)	(7)	(8)	(9)
(0) Axé	**83.33**	0.00	1.11	0.00	0.00	0.00	6.67	3.33	5.56	0.00
(1) Bachata	2.22	**93.33**	2.22	1.11	0.00	0.00	0.00	1.11	0.00	0.00
(2) Bolero	1.11	0.00	**91.11**	1.11	0.00	0.00	0.00	1.11	4.44	1.11
(3) Forró	2.22	1.11	4.44	**82.22**	6.67	0.00	0.00	2.22	1.11	0.00
(4) Gaúcha	14.44	0.00	6.67	6.67	**67.78**	0.00	0.00	0.00	4.44	0.00
(5) Merengue	0.00	3.33	1.11	0.00	0.00	**95.56**	0.00	0.00	0.00	0.00
(6) Pagode	6.67	0.00	11.11	0.00	1.11	0.00	**71.11**	3.33	6.67	0.00
(7) Salsa	7.78	0.00	4.44	0.00	3.33	0.00	0.00	**84.44**	0.00	0.00
(8) Sertaneja	11.11	1.11	8.89	1.11	7.78	0.00	2.22	0.00	**67.78**	0.00
(9) Tango	1.11	0.00	11.11	1.11	0.00	0.00	0.00	0.00	0.00	**86.67**

5.4 Brodatz-32 texture classification task

We now consider a classical problem in texture classification - the Brodatz-32 texture classification task. This dataset is significantly smaller than the other datasets tested in the present work, and it is used to evaluate how the proposed method performs on tasks with smaller datasets.

The images of the dataset are of size 64 x 64 pixels, and with such small size we did not consider resizing the image. Similarly to the other datasets, we run models with different hyperparameters and compare the results on the next sections. Training a Convolutional Network on the brodatz-32 dataset took about 2 minutes.

5.4.1 Classification rates

Figure 5.16 reports the error rates of the models trained on different hyperparameters.

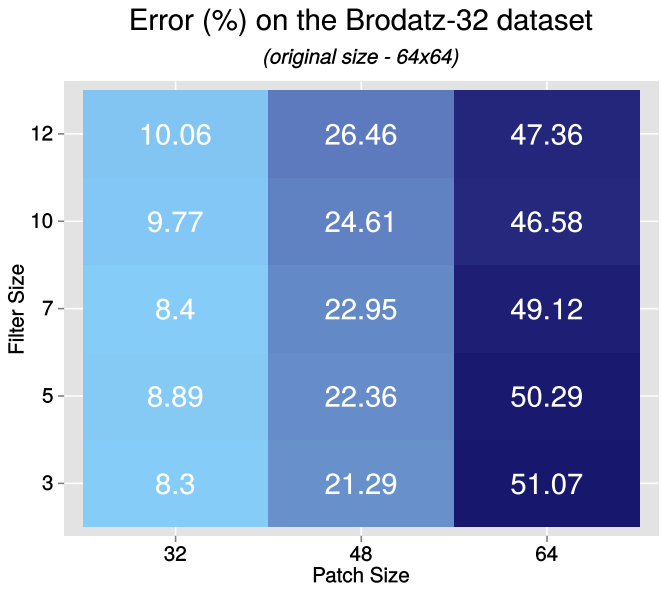

Figure 5.16: Error rates on the Brodatz dataset, for CNNs trained with different hyperparameters.

It is worth noting that for patches of size 48x48 and 64x64 we have only a single patch to classify the image, where patches of size 32x32 allowed the combination of 4 patches on each test image. The model with best performance was trained with Filter size of 3x3 and Patch size of 32x32. It is also interesting to observe that the models trained with patches of size 48x48 performed better than the patches of size 64x64, in spite of the fact that only a single patch is available per test image (in both cases). One hypothesis for this result is that, in the model trained with 48x48 patches, we use random patches during training, which may reduce the overfitting on the training data. We cannot use random patches for the model trained with 64x64 patches, since the images themselves are of size 64x64.

Figure 5.17 displays eight random patches from the testing set, from the network that obtained the best results above. Again, the image displays the probability assigned by the model to different classes (the 4 classes with higher probability), and the bar in red indicates the correct label (also shown below the image).

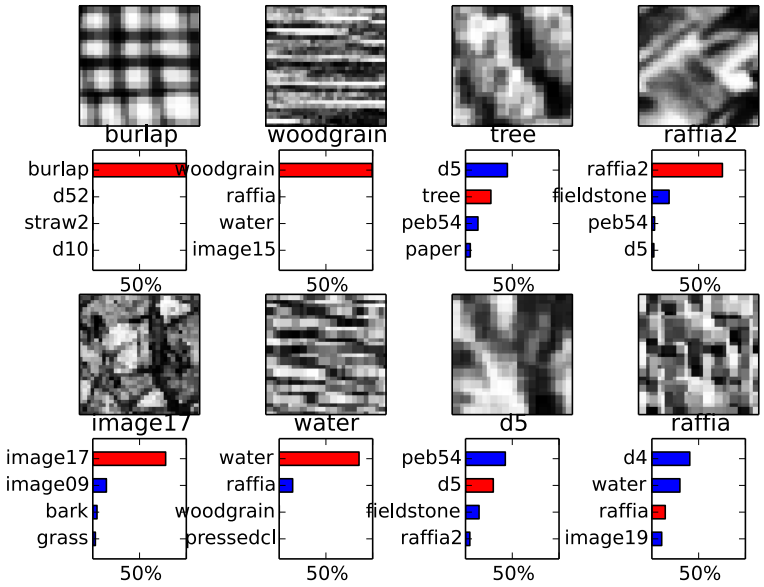

Figure 5.17: Random predictions for patches on the Brodatz-32 Testing set

5.4.2 Feature Learning

The filters learned by the first convolutional layer are displayed in Figure 5.18. In this case, we can see that only a few filters learned relevant features, while many of them remained very homogeneous (almost completely gray), and very redundant. This is likely due to low amount of data in the training set for this task.

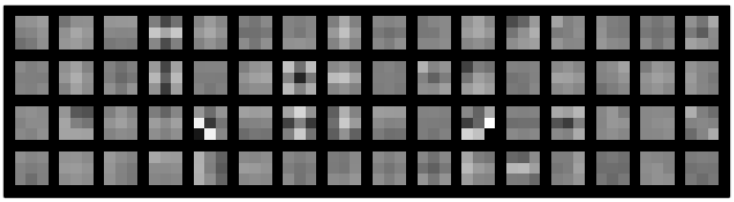

Figure 5.18: Filters learned by the first convolutional layer of a model trained on the Brodatz-32 dataset.

5.4.3 Comparison with the state of the art

Table 5.8 compare our results with the best published results in the Brodatz-32 task. The best published result for the Brodatz-32 dataset is from Chen [62] achieving 98.9% of accuracy on the 32-class classification problem using a novel LBP operator called Robust Local Binary Pattern. For this task, the proposed method achieves inferior results, with a mean accuracy of 91.27%.

Table 5.8: Classification on the Brodatz-32 dataset

Features and Algorithm	Accuracy
Gabor filters (KNN) [62]	95.8%
Multiple texture descriptors (Decision Trees) [63]	96.5%
Dominant LBP (KNN) [62]	98.30%
Robust LBP (KNN) [62]	**98.90**%
Proposed method (CNN)	91.27% (+- 0.53%)

5.5 Transfer Learning

We now present the results of our experiments with Transfer Learning. As presented in Chapter 4, our objective is to use one dataset to train a Convolutional Neural Network, and transfer knowledge to another task, seeking to improve the results on it.

For each experiment, we follow the procedure defined in Chapter 4: we first trained a Convolutional Neural Network on the source task, using the best hyperparameters from the results above. Then we use this model to obtain a new representation of the target dataset, projecting the samples to another feature space. Finally, we use this new representation of the target dataset to train a model. In these experiments, we trained Logistic Regression models and Support Vector Machines (SVMs). For the SVM training, we use the python package scikit-learn [64], that provides a wrapper over the libsvm [65] library. We train SVMs with the radial basis function (RBF) kernel, selecting the hyperparameters C and γ using a grid search, following the recommended values from Hsu [66]. It is worth noting that due to limitations on computing power, we do not optimize these hyperparameters using the whole training set. Instead, a subset of five thousand examples is randomly selected to perform this optimization, and subsequently an SVM is trained with these hyperparameters on the whole training set. We then test the model once in the testing set, and report the results.

5.5.1 Tasks from similar domains

We first present the results of transferring learning across tasks with similar domains. In particular, we selected two tests to perform: transfer learning across tasks on Forest species recognition (using the Microscopic and Macroscopic datasets), and transfer

learning across tasks on author identification (using the IAM and BFL datasets).

The first experiment involved the datasets for Forest species recognition. We used the dataset of Microscopic images to train a CNN, seeking to improve the performance on the task of recognizing the species from Macroscopic images. The results from this experiment are presented in Table 5.9.

Table 5.9: Classification on the Macroscopic Forest species dataset (using CNN trained on the Microscopic Forest species dataset)

Features and Algorithm	Accuracy
Multiple classifiers (SVM) [60]	**97.77**%
Proposed method (CNN)	**96.24**%
Transfer Learning (Logistic Regression)	93.76%
Transfer Learning (SVM)	95.55%

The best result using transfer learning achieved an accuracy of 95.55%, close to the best result obtained by training a CNN on the Macroscopic images dataset (96.24%). This suggests that, even though the images from both datasets look very different, the features learned for the dataset with Microscopic images were discriminative for the dataset with Macroscopic images. In particular, we can see that the result of Logistic Regression (a linear classifier) was reasonably high, and therefore the CNN (trained on the Microscopic dataset) is able to project the data from the Macroscopic dataset to a feature space where the classes are (almost) linearly separable.

For the second experiment with this strategy, we used a CNN trained on the IAM dataset, seeking to improve the results on the BFL dataset. The results for this experiment are presented in Table 5.10.

Table 5.10: Classification on the BFL dataset (using CNN trained on the IAM dataset)

Features and Algorithm	Accuracy
LPQ (SVM) [8]	**98.26**%
Proposed method (CNN)	95.36%
Transfer Learning (Logistic Regression)	**96.52**%
Transfer Learning (SVM)	93.91%

This experiment resulted in two interesting and unexpected results. Using Transfer Learning we were able to obtain a superior accuracy on the BFL dataset, compared

to the model trained with CNN directly. This suggests that the CNN trained on the IAM dataset learned features that are discriminative for the BFL dataset. The second unexpected result was that the SVM model presented worse results compared to the Logistic Regression model. We attribute this result to the fact that we do not optimize the SVM hyperparameters using the whole training set (130 thousand examples), but with a limited subset (5 thousand examples) due to limitations in computing power - even with 5 thousand examples, optimizing the hyperparameters C and γ took about 4 hours.

5.5.2 Tasks from distinct domains

We now consider experiments to transfer learning across tasks from different domains.

The first experiment was performed using the CNN trained on the Microscopic Forest species dataset, to improve the results on the BFL author identification dataset. We followed the same protocol defined in the methodology, obtaining the results in Table 5.11.

Table 5.11: Classification on the BFL dataset
(using CNN trained on the Microscopic Forest species dataset)

Features and Algorithm	Accuracy
LPQ (SVM) [8]	**98.26**%
Proposed method (CNN)	95.36%
Transfer Learning (Logistic Regression)	**95.65**%
Transfer Learning (SVM)	93.04%

The method using transfer learning achieved similar results from the method training a CNN directly on the BFL task. Since the model with Logistic Regression achieved good results, this suggests that the samples on the BFL dataset were projected to a feature space almost linearly-separable. We found this result surprising, since the datasets are very different in nature. We note, however, that these results were inferior to the Transfer Learning experiment using the IAM author identification dataset as source, suggesting that this strategy works better when we have similar tasks.

The last experiment was conducted using the same CNN (trained on the Microscopic

Forest species dataset) to increase the performance on the Brodatz-32 task. The results are presented in Table 5.12.

Table 5.12: Classification on the Brodatz-32 dataset
(using CNN trained on the Microscopic Forest images dataset)

Features and Algorithm	Accuracy
Robust LBP (KNN) [62]	**98.90**%
Proposed method (CNN)	91.27%
Transfer Learning (Logistic Regression)	93.85%
Transfer Learning (SVM)	**95.31**%

For this dataset, we could see a large increase in classification rate using the transfer learning method. This is likely due to the fact that the Brodatz-32 dataset is very small, and the CNN trained directly on it was unable to learn good representations. Even though the samples from the two datasets are very different, we can see that the representations learned by the CNN trained on the Microscopic Forest images dataset were relevant for the Brodatz-32 task. Considering the results on the experiments with the author identification datasets, we would expect even better results if the source task (used to train a CNN) was closer to the Brodatz-32 dataset, for example, a larger dataset of natural textures.

CHAPTER 6

CONCLUSION

The task of texture classification has relevant applications in a wide range of domains, and although being successful in many areas, it is still object of active research with potential to increase classification rates.

We developed a simple method to use Convolutional Neural Networks for texture classification, based on the methods used for object recognition, but taking advantage of the properties particular to texture classification. Our tests with six texture classification datasets demonstrated that this method is able to achieve state-of-the-art results in scenarios where large amounts of data are available, which is the case of many texture datasets (where large images are used).

We also presented a transfer learning method for texture classification using Convolutional Neural Networks, allowing the usage of a dataset from one classification task to improve the classification performance on other tasks. Our experiments with this strategy showed improved accuracy when using datasets from similar tasks. The experiments also demonstrated that this method can be used to improve the performance on tasks where the dataset is very small, by leveraging the knowledge learned by other texture classification tasks, even if they are not very similar.

Future work can explore the optimization of the hyperparameters on the convolutional network (such as number of layers, number of neurons per layer, etc.), since these hyperparamenters were fixed during the experiments on the present work. The strategy to extract patches during testing can also be further explored, experimenting with different strategies such as random patch extraction.

APPENDIX A

SAMPLE IMAGES ON THE DATASETS

As reviewed in Chapter 3, a total of six datasets were selected for this work. The datasets were selected to represent distinct domains, and to present different challenges for training. The figures below contain samples of each dataset:

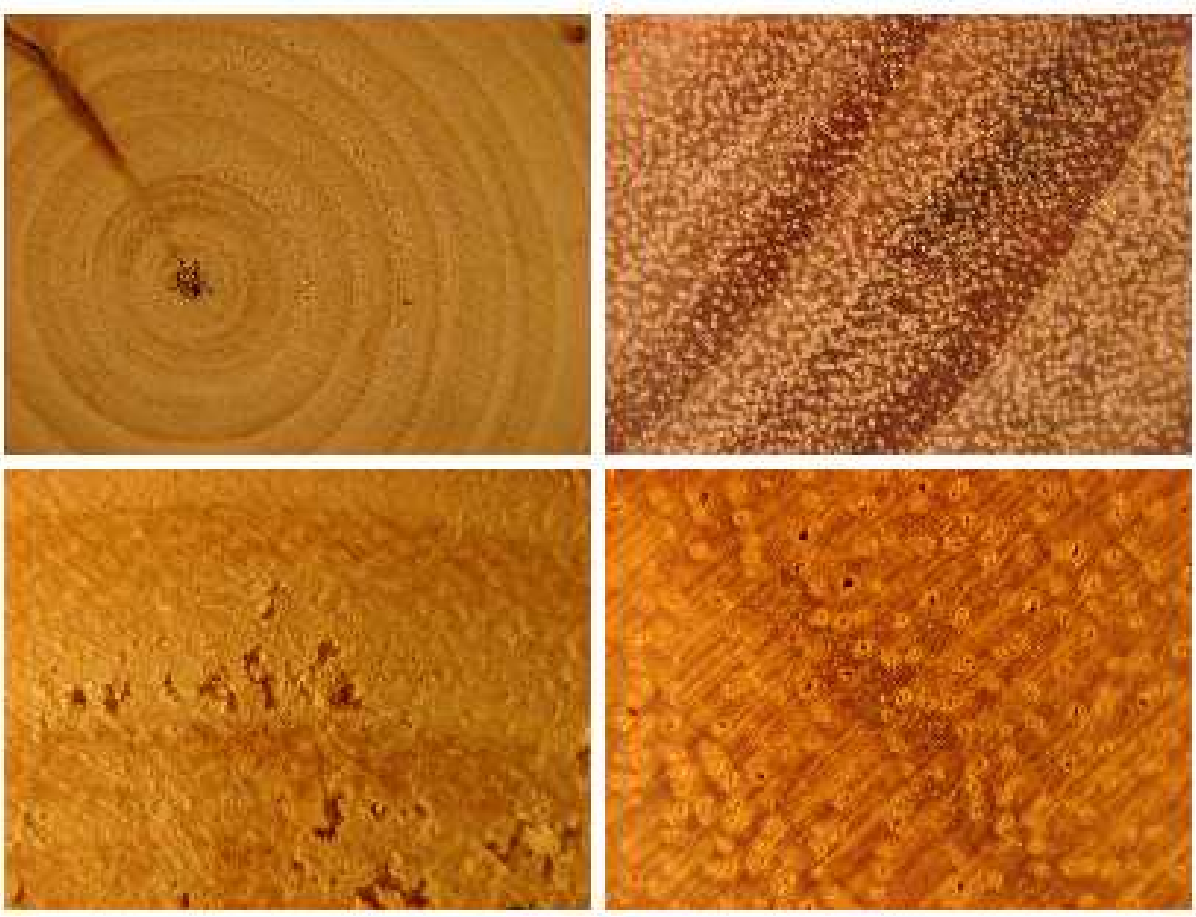

Figure A.1: Sample images from the macroscopic Brazilian forest species dataset

Figure A.2: Sample images from the microscopic Brazilian forest species dataset

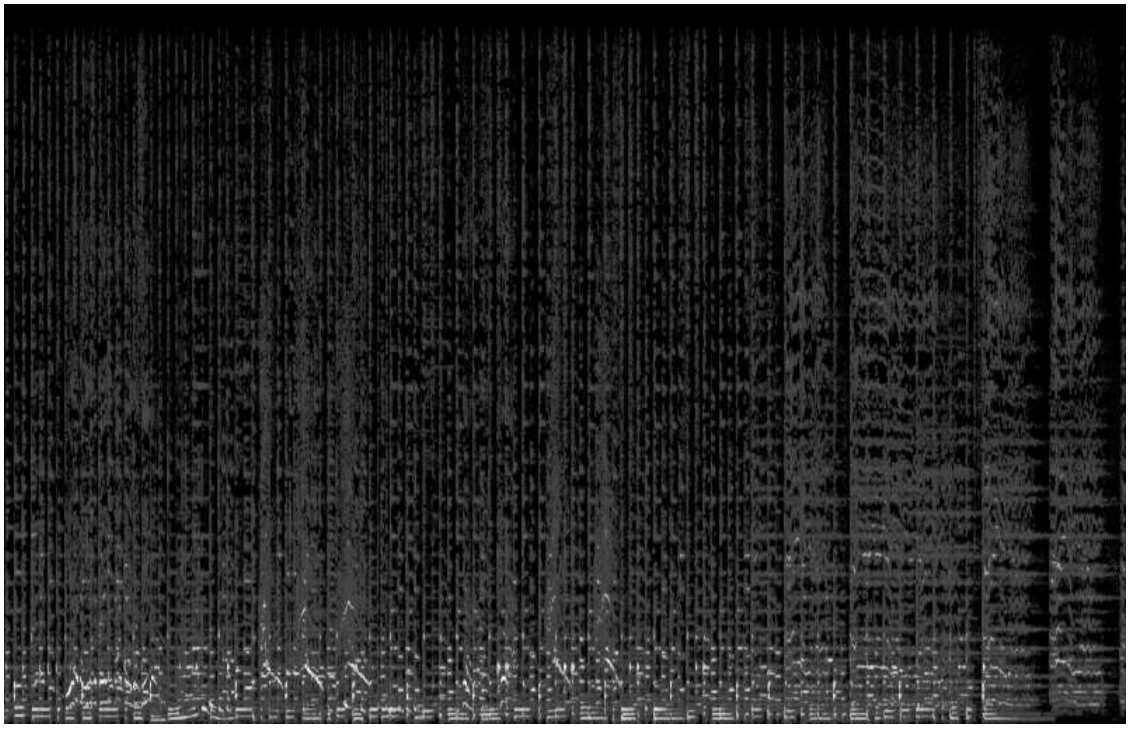

Figure A.3: Sample texture created from the Latin Music Dataset dataset.

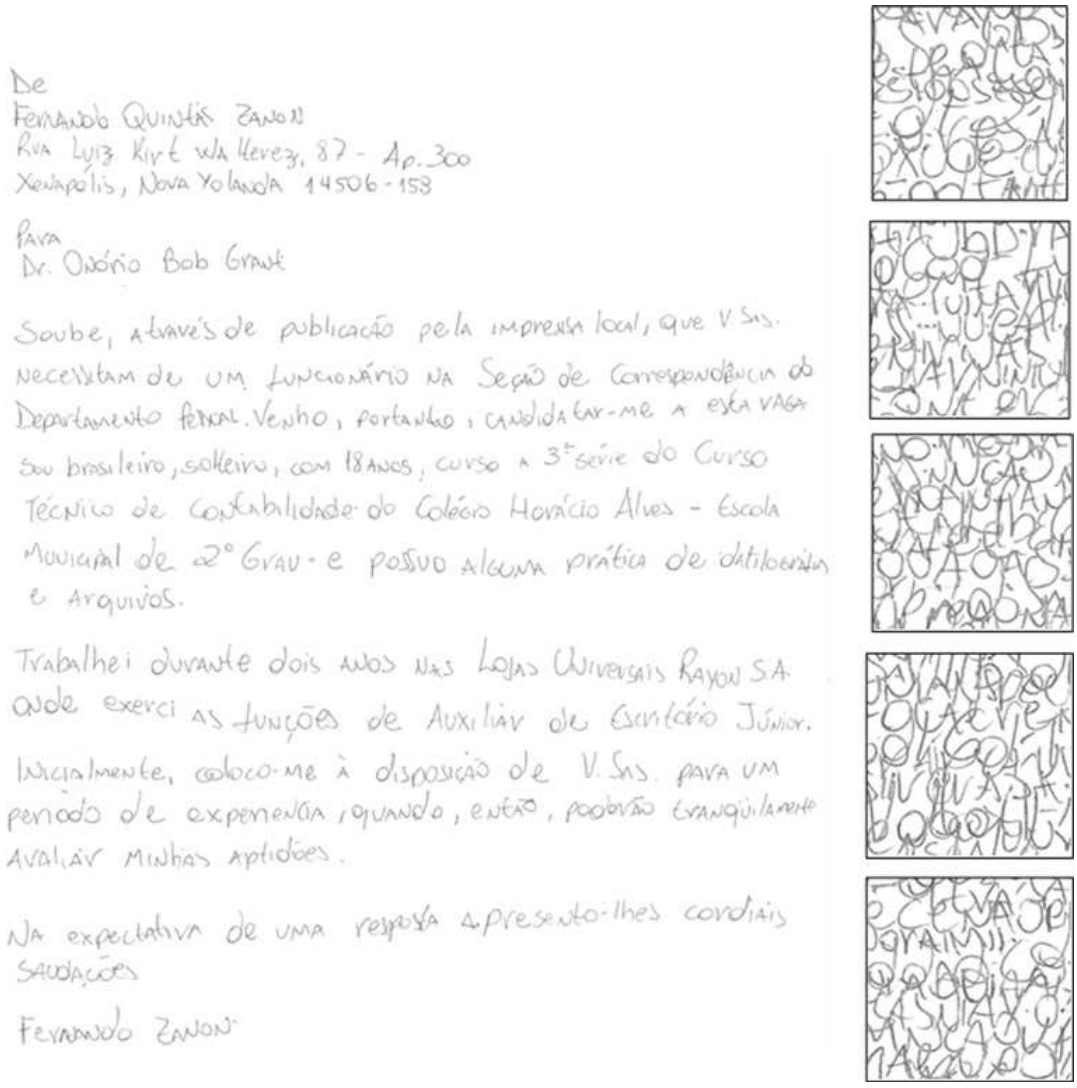

De
Fernando Quintas Zanon
Rua Luiz Kirt Wallerez, 87 - Ap. 300
Xenapólis, Nova Yolanda 14506-158

Para
Dr. Onório Bob Grant

Soube, através de publicação pela imprensa local, que V.Srs. necessitam de um funcionário na Seção de Correspondência do Departamento Pessoal. Venho, portanto, candidatar-me a esta vaga. Sou brasileiro, solteiro, com 18 anos, curso a 3ª série do Curso Técnico de Contabilidade do Colégio Horácio Alves - Escola Municipal de 2º Grau - e possuo alguma prática de datilografia e arquivos.

Trabalhei durante dois anos nas Lojas Universais Rayon S.A. onde exerci as funções de Auxiliar de Escritório Júnior.

Inicialmente, coloco-me à disposição de V. Srs. para um período de experiência, quando, então, poderão tranquilamente avaliar minhas aptidões.

Na expectativa de uma resposta, apresento-lhes cordiais saudações.

Fernando Zanon

Figure A.4: Sample image from the BFL dataset, and the associated texture. [53]

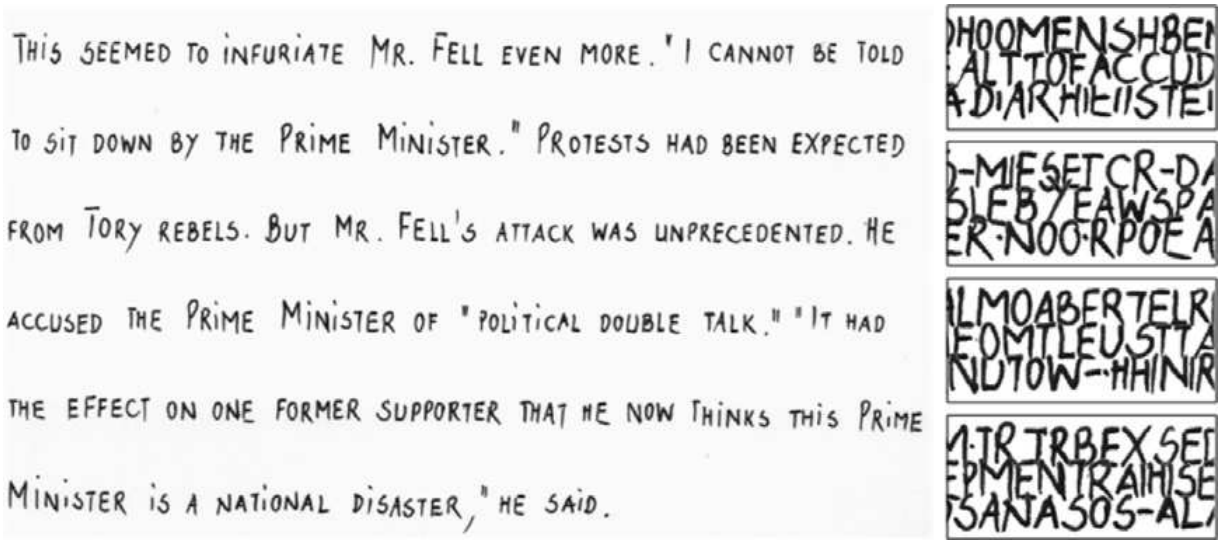

THIS SEEMED TO INFURIATE MR. FELL EVEN MORE. "I CANNOT BE TOLD TO SIT DOWN BY THE PRIME MINISTER." PROTESTS HAD BEEN EXPECTED FROM TORY REBELS. BUT MR. FELL'S ATTACK WAS UNPRECEDENTED. HE ACCUSED THE PRIME MINISTER OF "POLITICAL DOUBLE TALK." "IT HAD THE EFFECT ON ONE FORMER SUPPORTER THAT HE NOW THINKS THIS PRIME MINISTER IS A NATIONAL DISASTER," HE SAID.

Figure A.5: Sample image from the IAM dataset, and the associated texture. [8]

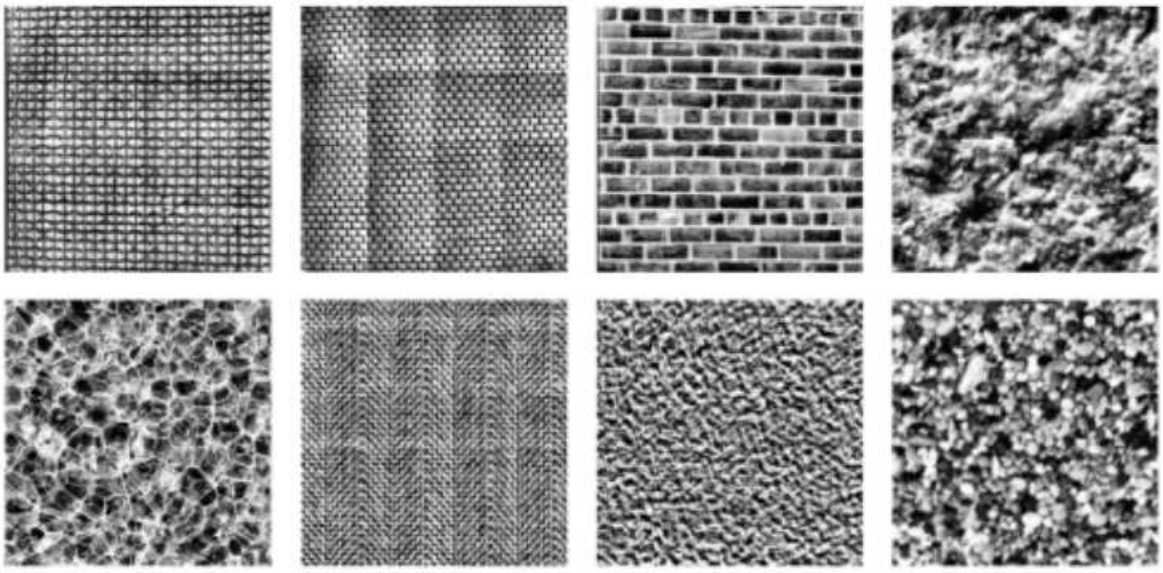

Figure A.6: Sample images from the Brodatz-32 dataset [58]

BIBLIOGRAPHY

[1] H. Harms, U. Gunzer, and H. M. Aus, "Combined local color and texture analysis of stained cells," *Computer Vision, Graphics, and Image Processing*, vol. 33, no. 3, pp. 364–376, Mar. 1986.

[2] A. Khademi and S. Krishnan, "Medical image texture analysis: A case study with small bowel, retinal and mammogram images," in *Canadian Conference on Electrical and Computer Engineering, 2008. CCECE 2008*, May 2008, pp. 001 949–001 954.

[3] R. Sutton and E. L. Hall, "Texture measures for automatic classification of pulmonary disease," *IEEE Transactions on Computers*, vol. C-21, no. 7, pp. 667–676, Jul. 1972.

[4] J. Y. Tou, Y. Tay, and P. Y. Lau, "A comparative study for texture classification techniques on wood species recognition problem," in *Fifth International Conference on Natural Computation, 2009. ICNC '09*, vol. 5, 2009, pp. 8–12.

[5] P. Filho, L. Oliveira, A. Britto, and R. Sabourin, "Forest species recognition using color-based features," in *2010 20th International Conference on Pattern Recognition (ICPR)*, 2010, pp. 4178–4181.

[6] M. Nasirzadeh, A. Khazael, and M. bin Khalid, "Woods recognition system based on local binary pattern," in *2010 Second International Conference on Computational Intelligence, Communication Systems and Networks (CICSyN)*, 2010, pp. 308–313.

[7] R. Haralick, K. Shanmugam, and I. Dinstein, "Textural features for image classification," *IEEE Transactions on Systems, Man and Cybernetics*, vol. SMC-3, no. 6, pp. 610–621, Nov. 1973.

[8] D. Bertolini, L. S. Oliveira, E. Justino, and R. Sabourin, "Texture-based descriptors for writer identification and verification," *Expert Systems with Applications*, 2012.

[9] Y. M. Costa, L. S. Oliveira, A. L. Koerich, F. Gouyon, and J. G. Martins, "Music genre classification using LBP textural features," *Signal Processing*, vol. 92, no. 11, p. 27232737, 2012.

[10] C. M. Bishop and N. M. Nasrabadi, *Pattern recognition and machine learning*. springer New York, 2006, vol. 1.

[11] J. Zhang and T. Tan, "Brief review of invariant texture analysis methods," *Pattern recognition*, vol. 35, no. 3, p. 735747, 2002.

[12] Y. Guo, G. Zhao, and M. Pietikinen, "Discriminative features for texture description," *Pattern Recognition*, vol. 45, no. 10, pp. 3834–3843, Oct. 2012.

[13] Y. Bengio, "Learning deep architectures for AI," *Foundations and trends in Machine Learning*, vol. 2, no. 1, p. 1127, Jan. 2009.

[14] G. E. Hinton, S. Osindero, and Y.-W. Teh, "A fast learning algorithm for deep belief nets," *Neural computation*, vol. 18, no. 7, pp. 1527–1554, 2006.

[15] Y. Bengio, P. Lamblin, D. Popovici, and H. Larochelle, "Greedy layer-wise training of deep networks," 2006.

[16] Y. Bengio and A. Courville, "Deep learning of representations," in *Handbook on Neural Information Processing*. Springer, 2013, pp. 1–28.

[17] A. Krizhevsky and G. Hinton, "Learning multiple layers of features from tiny images," Master's thesis, Department of Computer Science, University of Toronto, 2009.

[18] D. Ciresan, U. Meier, and J. Schmidhuber, "Multi-column deep neural networks for image classification," in *2012 IEEE Conference on Computer Vision and Pattern Recognition (CVPR)*, 2012, pp. 3642–3649.

[19] J. J. Kivinen and C. Williams, "Multiple texture boltzmann machines," in *International Conference on Artificial Intelligence and Statistics*, 2012, pp. 638–646.

[20] H. Luo, P. L. Carrier, A. Courville, and Y. Bengio, "Texture modeling with convolutional spike-and-slab rbms and deep extensions," in *Proceedings of the Sixteenth International Conference on Artificial Intelligence and Statistics*, 2013, pp. 415–423.

[21] F. H. C. Tivive and A. Bouzerdoum, "Texture classification using convolutional neural networks," in *TENCON 2006. 2006 IEEE Region 10 Conference*. IEEE, 2006, pp. 1–4.

[22] Q. V. Le, "Building high-level features using large scale unsupervised learning," in *Acoustics, Speech and Signal Processing (ICASSP), 2013 IEEE International Conference on*. IEEE, 2013, pp. 8595–8598.

[23] J. A. Hertz, A. S. Krogh, and R. G. Palmer, *Introduction to the Theory of Neural Computacion*. Basic Books, 1991, vol. 1.

[24] W. S. McCulloch and W. Pitts, "A logical calculus of the ideas immanent in nervous activity," *The Bulletin of Mathematical Biophysics*, vol. 5, no. 4, p. 115133, 1943.

[25] D. E. Rumelhart, G. E. Hintont, and R. J. Williams, "Learning representations by back-propagating errors," *Nature*, vol. 323, no. 6088, pp. 533–536, 1986.

[26] A. Krizhevsky, I. Sutskever, and G. E. Hinton, "ImageNet classification with deep convolutional neural networks." in *NIPS*, vol. 1, 2012, p. 4.

[27] M. Minsky and S. Papert, *Perceptrons : an introduction to computational geometry*. MIT, 1969.

[28] K. Hornik, M. Stinchcombe, and H. White, "Multilayer feedforward networks are universal approximators," *Neural networks*, vol. 2, no. 5, p. 359366, 1989.

[29] P. Golik, P. Doetsch, and H. Ney, "Cross-entropy vs. squared error training: a theoretical and experimental comparison." in *INTERSPEECH*, 2013, p. 17561760.

[30] Y. LeCun, L. Bottou, Y. Bengio, and P. Haffner, "Gradient-based learning applied to document recognition," *Proceedings of the IEEE*, vol. 86, no. 11, p. 22782324, 1998.

[31] E. Alpaydin, *Introduction to machine learning.* MIT press, 2004.

[32] R. O. Duda, P. E. Hart, and D. G. Stork, *Pattern classification.* John Wiley & Sons, 1999.

[33] H. Larochelle, D. Erhan, A. Courville, J. Bergstra, and Y. Bengio, "An empirical evaluation of deep architectures on problems with many factors of variation," in *Proceedings of the 24th international conference on Machine learning.* ACM, 2007, p. 473480.

[34] D. Erhan, P.-A. Manzagol, Y. Bengio, S. Bengio, and P. Vincent, "The difficulty of training deep architectures and the effect of unsupervised pre-training," in *International Conference on Artificial Intelligence and Statistics*, 2009, p. 153160.

[35] O. Russakovsky, J. Deng, H. Su, J. Krause, S. Satheesh, S. Ma, Z. Huang, A. Karpathy, A. Khosla, M. Bernstein, A. C. Berg, and L. Fei-Fei, "ImageNet large scale visual recognition challenge," *arXiv:1409.0575 [cs]*, Sep. 2014, arXiv: 1409.0575.

[36] D. Ciresan, U. Meier, J. Masci, and J. Schmidhuber, "A committee of neural networks for traffic sign classification," in *Neural Networks (IJCNN), The 2011 International Joint Conference on.* IEEE, 2011, p. 19181921.

[37] Y. LeCun, B. Boser, J. S. Denker, D. Henderson, R. E. Howard, W. Hubbard, and L. D. Jackel, "Backpropagation applied to handwritten zip code recognition," *Neural computation*, vol. 1, no. 4, p. 541551, 1989.

[38] D. Scherer, A. Mller, and S. Behnke, "Evaluation of pooling operations in convolutional architectures for object recognition," in *Artificial Neural NetworksICANN 2010.* Springer, 2010, p. 92101.

[39] J. Kittler, M. Hatef, R. P. W. Duin, and J. Matas, "On combining classifiers," *IEEE Transactions on Pattern Analysis and Machine Intelligence*, vol. 20, no. 3, pp. 226–239, 1998.

[40] S. J. Pan and Q. Yang, "A survey on transfer learning," *Knowledge and Data Engineering, IEEE Transactions on*, vol. 22, no. 10, pp. 1345–1359, 2010.

[41] M. Oquab, L. Bottou, I. Laptev, J. Sivic, and others, "Learning and transferring mid-level image representations using convolutional neural networks," INRIA, Tech. Rep. HAL-00911179, 2013.

[42] H. Lee, R. Grosse, R. Ranganath, and A. Y. Ng, "Convolutional deep belief networks for scalable unsupervised learning of hierarchical representations," in *Proceedings of the 26th Annual International Conference on Machine Learning*, ser. ICML '09. New York, NY, USA: ACM, 2009, p. 609616.

[43] R. Collobert and J. Weston, "A unified architecture for natural language processing: Deep neural networks with multitask learning," in *Proceedings of the 25th international conference on Machine learning*. ACM, 2008, p. 160167.

[44] A.-r. Mohamed, T. N. Sainath, G. Dahl, B. Ramabhadran, G. E. Hinton, and M. A. Picheny, "Deep belief networks using discriminative features for phone recognition," in *Acoustics, Speech and Signal Processing (ICASSP), 2011 IEEE International Conference on*. IEEE, 2011, p. 50605063.

[45] I. Goodfellow, D. Warde-farley, M. Mirza, A. Courville, and Y. Bengio, "Maxout networks," in *Proceedings of the 30th International Conference on Machine Learning (ICML-13)*, 2013, pp. 1319–1327.

[46] G. E. Hinton, N. Srivastava, A. Krizhevsky, I. Sutskever, and R. R. Salakhutdinov, "Improving neural networks by preventing co-adaptation of feature detectors," arXiv e-print 1207.0580, Jul. 2012.

[47] J. Snoek, H. Larochelle, and R. P. Adams, "Practical bayesian optimization of machine learning algorithms," arXiv e-print 1206.2944, Jun. 2012.

[48] M. D. Zeiler and R. Fergus, "Stochastic pooling for regularization of deep convolutional neural networks," in *ICLR*, 2013.

[49] P. L. de Paula Filho, L. S. Oliveira, and A. S. Britto Jr, "A database for forest species recognition," in *Proceedings of the XXII Brazilian Symposium on Computer Graphics and Image Processing*, 2009.

[50] P. Filho, "Reconhecimento de especies florestais atraves de imagens macroscopicas," Ph.D. dissertation, Universidade Federal do Parana, 2012.

[51] J. Martins, L. S. Oliveira, S. Nisgoski, and R. Sabourin, "A database for automatic classification of forest species," *Machine Vision and Applications*, vol. 24, no. 3, pp. 567–578, Apr. 2013.

[52] C. Freitas, L. S. Oliveira, R. Sabourin, and F. Bortolozzi, "Brazilian forensic letter database," in *11th International workshop on frontiers on handwriting recognition, Montreal, Canada*, 2008.

[53] R. K. Hanusiak, L. S. Oliveira, E. Justino, and R. Sabourin, "Writer verification using texture-based features," *International Journal on Document Analysis and Recognition (IJDAR)*, vol. 15, no. 3, p. 213226, 2012.

[54] U.-V. Marti and H. Bunke, "The IAM-database: an english sentence database for offline handwriting recognition," *International Journal on Document Analysis and Recognition*, vol. 5, no. 1, p. 3946, 2002.

[55] C. N. Silla Jr, A. L. Koerich, and C. A. Kaestner, "The latin music database." in *ISMIR*, 2008, p. 451456.

[56] Y. Costa, L. Oliveira, A. Koerich, and F. Gouyon, "Music genre recognition using gabor filters and lpq texture descriptors," in *Progress in Pattern Recognition, Image Analysis, Computer Vision, and Applications*. Springer, 2013, p. 6774.

[57] P. Brodatz, *Textures: a photographic album for artists and designers*. Dover New York, 1966, vol. 66.

[58] K. Valkealahti and E. Oja, "Reduced multidimensional co-occurrence histograms in texture classification," *IEEE Transactions on Pattern Analysis and Machine Intelligence*, vol. 20, no. 1, pp. 90–94, Jan. 1998.

[59] A. Coates, A. Y. Ng, and H. Lee, "An analysis of single-layer networks in unsupervised feature learning," in *International Conference on Artificial Intelligence and Statistics*, 2011, pp. 215–223.

[60] P. L. P. Filho, L. S. Oliveira, S. Nisgoski, and A. S. Britto, "Forest species recognition using macroscopic images," *Machine Vision and Applications*, Jan. 2014.

[61] P. R. Cavalin, M. N. Kapp, J. Martins, and L. E. S. Oliveira, "A multiple feature vector framework for forest species recognition," in *Proceedings of the 28th Annual ACM Symposium on Applied Computing*, ser. SAC '13. New York, NY, USA: ACM, 2013, pp. 16–20.

[62] J. Chen, V. Kellokumpu, G. Zhao, and M. Pietikinen, "RLBP: robust local binary pattern," in *Proceedings of the British Machine Vision Conference*. BMVC, 2013.

[63] E. Urbach, J. Roerdink, and M. Wilkinson, "Connected shape-size pattern spectra for rotation and scale-invariant classification of gray-scale images," *IEEE Transactions on Pattern Analysis and Machine Intelligence*, vol. 29, no. 2, pp. 272–285, 2007.

[64] F. Pedregosa, G. Varoquaux, A. Gramfort, V. Michel, B. Thirion, O. Grisel, M. Blondel, P. Prettenhofer, R. Weiss, V. Dubourg, J. Vanderplas, A. Passos, D. Cournapeau, M. Brucher, M. Perrot, and E. Duchesnay, "Scikit-learn: Machine learning in Python," *Journal of Machine Learning Research*, vol. 12, pp. 2825–2830, 2011.

[65] C.-C. Chang and C.-J. Lin, "LIBSVM: A library for support vector machines," *ACM Transactions on Intelligent Systems and Technology*, vol. 2, pp. 27:1–27:27, 2011, software available at http://www.csie.ntu.edu.tw/ cjlin/libsvm.

[66] C.-W. Hsu, C.-C. Chang, C.-J. Lin *et al.*, "A practical guide to support vector classification," 2003.

LUIZ GUSTAVO HAFEMANN

AN ANALYSIS OF DEEP NEURAL NETWORKS FOR TEXTURE CLASSIFICATION

Dissertation presented as partial requisite to obtain the Master's degree. M.Sc. program in Informatics, Universidade Federal do Paraná.
Advisor: Prof. Dr. Luiz Eduardo S. de Oliveira
Co-Advisor: Dr. Paulo Rodrigo Cavalin

CURITIBA

2014